

MICROCOPY RESOLUTION TEST CHART
NATIONAL BUREAU OF STANDARDS-1963-A

2

AIR FORCE OFFICE OF SCIENTIFIC RESEARCH (AFSC)
NOTICE OF TRANSMITTAL TO DTIC
This technical report has been reviewed and is
approved for public release IAW AFR 190-12.
Distribution is unlimited.
MATTHEW J. KEPNER
Chief, Technical Information Division

AD-A174 572

AFOSR-TR- 86 - 1094

Approved for public release;
distribution unlimited.

THIN-FILM
OPTOELECTRONIC CIRCUITS
RESEARCH PROGRAM

Annual Technical Report
on
AFOSR Contract No. F49629-85-C-0050

by
Steven M. Arnold

July 1986

Honeywell Physical Sciences Center
10701 Lyndale Avenue South
Bloomington, Minnesota 55420

DTIC
ELECTE
NOV 26 1986
S D

DTIC FILE COPY

Honeywell

86 11 25 272

UNCLASSIFIED

SECURITY CLASSIFICATION OF THIS PAGE

REPORT DOCUMENTATION PAGE				
1a. REPORT SECURITY CLASSIFICATION Unclassified		1b. RESTRICTIVE MARKINGS		
2a. SECURITY CLASSIFICATION AUTHORITY		3. DISTRIBUTION / AVAILABILITY OF REPORT Approved for public release: distribution unlimited		
2b. DECLASSIFICATION / DOWNGRADING SCHEDULE				
4. PERFORMING ORGANIZATION REPORT NUMBER(S)		5. MONITORING ORGANIZATION REPORT NUMBER(S) AFOSR-TR-86-1094		
6a. NAME OF PERFORMING ORGANIZATION Honeywell Physical Sciences Center	6b. OFFICE SYMBOL (if applicable)	7a. NAME OF MONITORING ORGANIZATION USAF, AFSC Air Force Office of Scientific Research		
6c. ADDRESS (City, State, and ZIP Code) 10701 Lyndale Avenue South Bloomington, MN 55420		7b. ADDRESS (City, State, and ZIP Code) Bldg. 410 Bolling AFB, Washington, D.C. 20332		
8a. NAME OF FUNDING / SPONSORING ORGANIZATION AFOSR	8b. OFFICE SYMBOL (if applicable) NE	9. PROCUREMENT INSTRUMENT IDENTIFICATION NUMBER F49629-85-C-0050		
8c. ADDRESS (City, State, and ZIP Code) Same as 7b		10. SOURCE OF FUNDING NUMBERS		
		PROGRAM ELEMENT NO. 61102F	PROJECT NO. 2305	TASK NO. B1
		WORK UNIT ACCESSION NO.		
11. TITLE (Include Security Classification) Thin Film Optoelectronic Circuits Research Program (Unclassified)				
12. PERSONAL AUTHOR(S) Steven M. Arnold				
13a. TYPE OF REPORT Annual Technical	13b. TIME COVERED FROM 85/2/1 TO 86/6/30	14. DATE OF REPORT (Year, Month, Day) 86/7/25	15. PAGE COUNT 50	
16. SUPPLEMENTARY NOTATION				
17. COSATI CODES			18. SUBJECT TERMS (Continue on reverse if necessary and identify by block number)	
FIELD	GROUP	SUB-GROUP	Integrated Optics Electro-Optic Devices	
			Gallium Arsenide (GaAs) Thin Film Waveguides	
			Zinc Oxide (ZnO)	
19. ABSTRACT (Continue on reverse if necessary and identify by block number) The program objective is to identify and investigate IC-compatible fabrication processes for thin film optoelectronic circuits on GaAs. Single mode channel waveguides of SiO ₂ -ZnO-SiO ₂ and SiO ₂ -Al ₂ O ₃ -SiO ₂ have been deposited on GaAs by ion beam sputtering. Straight guides, curves, tapers, Y-branches, crossovers, and directional couplers have all been demonstrated. Novel concepts have been developed for integrated GaAs Schottky photodiodes and self-aligning fiber-to-waveguide couplers. An IC-compatible baseline fabrication process has been established and a photomask set has been completed for an optoelectronic circuit demonstration. This demonstration circuit will include Mach-Zehnder interferometric modulators, delta-beta electro-optic switches, and integrated GaAs photodetectors.				
20. DISTRIBUTION / AVAILABILITY OF ABSTRACT <input type="checkbox"/> UNCLASSIFIED/UNLIMITED <input checked="" type="checkbox"/> SAME AS RPT <input type="checkbox"/> DTIC USERS		21. ABSTRACT SECURITY CLASSIFICATION Unclassified		
22a. NAME OF RESPONSIBLE INDIVIDUAL Giles		22b. TELEPHONE (Include Area Code) 767-4931	22c. OFFICE SYMBOL NE	

DD FORM 1473, 84 MAR

83 APR edition may be used until exhausted
All other editions are obsolete.

SECURITY CLASSIFICATION OF THIS PAGE

Unclassified

**THIN-FILM
OPTOELECTRONIC CIRCUITS
RESEARCH PROGRAM**

Annual Technical Report
on
AFOSR Contract No. F49629-85-C-0050

by
Steven M. Arnold

July 1986

Honeywell Physical Sciences Center
10701 Lyndale Avenue South
Bloomington, Minnesota 55420



Accession For	
NTIS CRA&I	<input checked="" type="checkbox"/>
DTIC TAB	<input type="checkbox"/>
Unannounced	<input type="checkbox"/>
Justification	
By _____	
Distribution /	
Availability Codes	
Dist	Avail and/or Special
A-1	

Approved by:

Alfman
Anis Husain, Section Head

Norm Foss
Norm Foss, Department Manager

Date:

7/28/86

Date:

7/28/86

Table of Contents

Section		Page
I	INTRODUCTION	1-1
	Statement of the Problem	1-1
	Zinc Oxide on Gallium Arsenide	1-1
	Summary of Approach	1-3
II	TECHNICAL OBJECTIVES	2-1
	Long-Term Objective	2-1
	Objectives of Current Program	2-1
III	STATUS OF THE RESEARCH EFFORT	3-1
	Zinc Oxide Material	3-1
	Waveguide Structures	3-1
	Fiber-to-Waveguide Coupling	3-10
	Electro-Optic Switches and Modulators	3-13
	Integrated Photodetectors	3-14
	Process Integration	3-16
	Summary of Accomplishments	3-18
IV	FUTURE PLAN OF THE PROGRAM	4-1
	Program Schedule	4-1
	Statement of Work	4-1
	Process Integration	4-1
	Optical Circuit Design and Layout	4-1
	Optical Circuit Fabrication	4-3
	Optical Circuit Testing and Evaluation	4-3
	Directions for Future Research	4-4
V	APPENDIX	5-1
	Key Personnel	5-1
	Publications	5-1
	Phase II Mask Set	5-2

List of Illustrations

Figure		Page
1-1	Thin-Film Waveguide Structure	1-3
1-2	Delta Beta Electro-Optic Switch	1-4
1-3	Mach-Zehnder Interferometric Switch	1-5
1-4	Fiber-to-Waveguide Coupling	1-6
1-5	Integrated Waveguide Photodetector	1-6
3-1	Channel Waveguide Fabrication Process	3-3
3-2	Photoresist Shadow Mask	3-4
3-3	Waveguide Ridge	3-4
3-4	Modes of ZnO Thin-Film Waveguide	3-5
3-5	Dependence of Ridge Height on Channel Width	3-6
3-6	Computer Plot of Channel Waveguide Mask	3-8
3-7	Photos of Channel Waveguide Mask	3-9
3-8	Thin-Film Channel Waveguides	3-9
3-9	Waveguide Evaluation Facility	3-10
3-10	Dependence of Mode Dimension on ZnO Film Thickness	3-12
3-11	Fiber-to-Waveguide Mode Matching	3-13
3-12	Integrated Photodetector for Channel Waveguides	3-14
3-13	I-V Characteristic of Schottky Photodetector	3-15
3-14	Optical Circuit Fabrication Process	3-17
4-1	Phase II Program Schedule	4-2
5-1	Program Organization	5-1
5-2	Computer Plots of Phase II Mask Set	5-3

List of Tables

Table		Page
1-1	Electro-Optic Waveguide Materials	1-2
4-1	Phase II Processing Runs	4-3

Section I INTRODUCTION

STATEMENT OF THE PROBLEM

Monolithic integration of electronic circuits in silicon has made possible a revolution in electronic computation and signal processing. Today, gallium arsenide integrated circuits (GaAs ICs) are extending this electronic revolution to ever higher speed devices.

Optical signal processing, despite its consistent advances and several early successes such as synthetic aperture radar and the optical spectrum analyzer, is falling increasingly behind the electronic competition. Functions which formerly required the speed and parallelism of optics are now being implemented entirely in digital electronics. The reasons for this are several, but one in particular stands out: the lack of emphasis given to compatibility issues between optical and electronic IC fabrication processes. As a result, most integrated optic devices demonstrated to date have been discrete components requiring laborious interfacing to predominantly electronic systems.

For integrated optical signal processors to compete on a cost basis with digital electronics, monolithic optoelectronic integration will be required. Optical waveguides, switches, modulators, sources and detectors as well as electronics must be integrated on a single substrate. Electronics, being the dominant technology, will not likely bend to accommodate the optics. Therefore integrated optics must seek better compatibility with mainstream electronics.

ZINC OXIDE ON GALLIUM ARSENIDE

Honeywell's approach to IC compatible optoelectronic integration uses thin-film waveguides of zinc oxide (ZnO) on substrates of gallium arsenide. Table 1-1 offers a comparison of thin-film ZnO with two more prevalent waveguide materials -- lithium niobate (LiNbO₃) and aluminum gallium arsenide (AlGaAs).

LiNbO₃ is the current research material of choice for integrated optics. It is reasonably transparent and has strong electro-optic and piezoelectric properties. Channel waveguides are fabricated in LiNbO₃ by in-diffusion of titanium. The resulting waveguides have rather large mode dimensions which can be well matched to optical fibers. A number of researchers have demonstrated impressive integrated optic devices in LiNbO₃. The chief disadvantage of LiNbO₃ is that it offers no possibilities for monolithic integration of detectors, electronics or light sources. Also, coupling of LiNbO₃ devices to other optical components requires expensive polishing and alignment operations.

Table 1-1. Electro-Optic Waveguide Materials

Property	Material		
	Thin Film ZnO	LiNbO ₃	AlGaAs on GaAs
Fabrication Method	Sputtered film	Ti diffusion	Epitaxial growth
Refractive Index	2.0	2.2	3.5
Attenuation	> 0.1 dB/cm	> 0.5 dB/cm	4 to 40 dB/cm
Electro-Optic Coefficient (10 ⁻¹² m/V)	r ₁₃ = -1.4 r ₃₃ = +2.6	r ₁₃ = +8.6 r ₃₃ = +30.8	r ₄₁ = -1.5
Piezoelectric Effect	Moderate	Strong	Very weak
Fiber Coupling Method	Vee-groove	Polish & align	Vee-groove
Mode Matching to Fiber	More difficult	Easy	More difficult
Electronics Compatible?	Yes	No	Yes, but...
Laser Compatible?	Yes, on GaAs	No	Yes
First Lab Demo	1969	1974	1970
3-inch Wafer Cost	\$ 7	\$ 200	\$ 250

AlGaAs is often cited as a material system permitting full monolithic integration of high-speed electronics, optical waveguides and diode lasers. Honeywell was the first to demonstrate the monolithic integration of an AlGaAs transverse junction stripe (TJS) laser with a GaAs 4:1 multiplexer. Such full optoelectronic integration is very difficult because the electronic properties of the material are degraded by the high temperature processes required for growing lasers and waveguides. Also, AlGaAs waveguides have rather high optical loss.

Deposited waveguides of ZnO or other thin-film materials have a number of advantages over either bulk crystal (LiNbO₃) or epitaxially grown (AlGaAs) waveguides. Thin films can be sputter deposited inexpensively on a variety of substrates including both Si and GaAs. The sputtering is done at relatively low temperatures, permitting the fabrication of electronics and/or lasers on the same substrate. Because of their lower optical loss and lower temperature of deposition, thin-film waveguides are an attractive alternative to AlGaAs waveguides for monolithic integration on GaAs.

Similarity of mode profiles and ease of alignment are important considerations when coupling integrated optical devices to optical fibers or diode lasers. Compared to LiNbO₃ waveguides, the mode profiles of thin-film waveguides are less well matched to those of optical fibers but better matched to diode lasers. Precise vee-grooves

can be anisotropically etched into substrates of Si or GaAs, thus providing inexpensive alignment between thin-film waveguides and optical fibers.

Zinc oxide is a unique thin-film waveguide material. Sputter deposited ZnO films are polycrystalline with the c-axis oriented normal to the substrate. ZnO has sizeable piezo-electric, electro-optic, and nonlinear optical coefficients, making it possible to fabricate surface acoustic wave (SAW) and active optical devices in the same film. Waveguides of ZnO can have very low optical losses, with values as low as 0.01 dB/cm having been reported for laser annealed planar films on oxidized silicon.

SUMMARY OF APPROACH

The following several paragraphs summarize the basic optical components (waveguides, switches, couplers and detectors) required for fabricating thin-film ZnO on GaAs optoelectronic circuits.

The structure of our thin-film channel waveguides is depicted in Figure 1-1. Light is confined to the ZnO film which is sandwiched between two lower index layers of SiO₂. For single mode operation, the thickness of the ZnO layer is about 0.3 micron while the lower SiO₂ (buffer) layer must be 1.0 micron or more to minimize coupling to the higher index substrate. While waveguides on Si have generally used a thermally grown buffer layer, GaAs substrates necessarily require a deposited oxide. A second oxide layer, deposited over the ZnO, provides passivation and a symmetric mode structure.

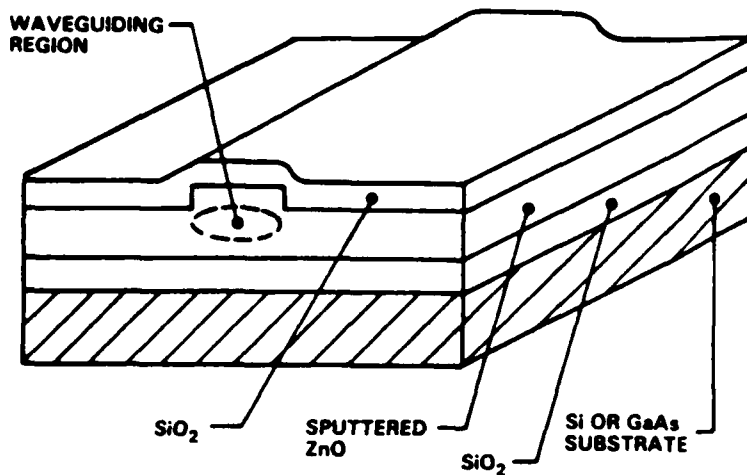


Figure 1-1. Thin-Film Waveguide Structure. Vertical confinement is provided by the planar SiO₂-ZnO-SiO₂ structure. Thicker ZnO in the channel region produces lateral confinement by locally increasing the effective refractive index.

Lateral confinement of the optical mode is provided by ridge structure which increases the effective refractive index in the channel region. Various combinations of ridge height and width will result in single mode waveguides, but a width of 2.5 microns and a height of about 100 Å provide a good compromise between ease of fabrication and acceptable bending losses. Since the ridge height is rather small, scattering due to sidewall roughness can be minimal.

An electro-optic switch of the 4-port directional coupler delta beta type is depicted in Figure 1-2. This type of switch can be readily fabricated in ZnO waveguides and is useful for crossbar networks and other applications in which light must be switched from one channel to another. The fraction of light coupled into the parallel guide is a periodic function of the interaction length. Generally, this length is chosen to be a bit longer than one half coupling period. A voltage across the electrodes produces equal and opposite refractive index changes (electro-optic effect) in the two guides. The resulting imbalance modifies the coupling. The split electrode configuration assures that the coupling can be electrically tuned between zero and 100 percent without the need for achieving exactly one half coupling period.

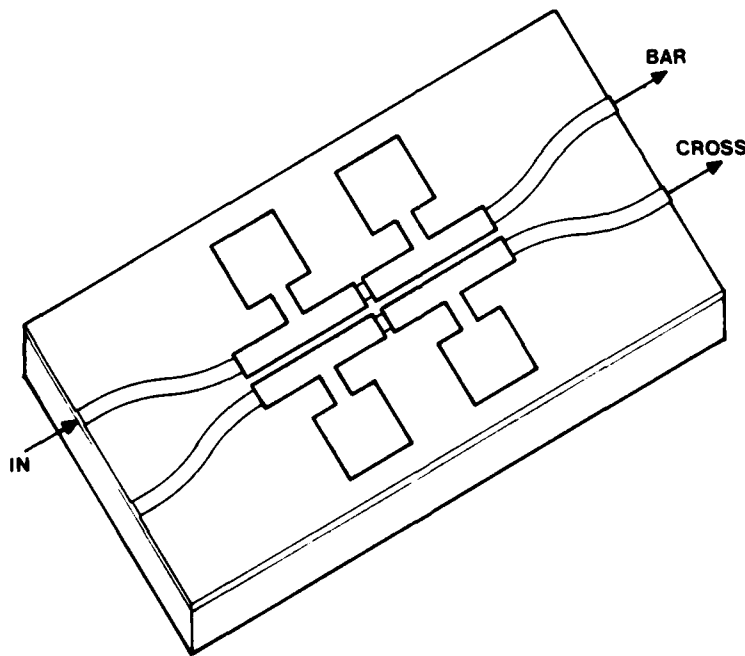


Figure 1-2. Delta Beta Electro-Optic Switch. Coupling between the two waveguides depends on their separation, length of interaction, and any differences in mode velocity (beta). Length and separation are chosen to give complete crossover. A voltage across the electrodes then unbalances the mode velocities to prevent crossover.

A second type of electro-optic switch, the Mach-Zehnder interferometer, is depicted in Figure 1-3. This is essentially an intensity modulator. A first Y-branch divides the light equally between the two legs of the interferometer. A second Y-branch then recombines the light following an electro-optic phase shift applied differentially between the two legs. The in-phase fraction of the light is coupled to the output guide while the out-of-phase portion is lost to radiation modes.

Figure 1-4 depicts the use of vee-grooves for automatic alignment of optical fibers to thin-film waveguides. The vee-grooves, bounded by slow etching 111 crystallographic planes, are obtained by anisotropic etching of the GaAs substrate. This approach is more production oriented than the lapping, polishing and micropositioning technique currently required for attaching fibers to LiNbO_3 integrated circuits.

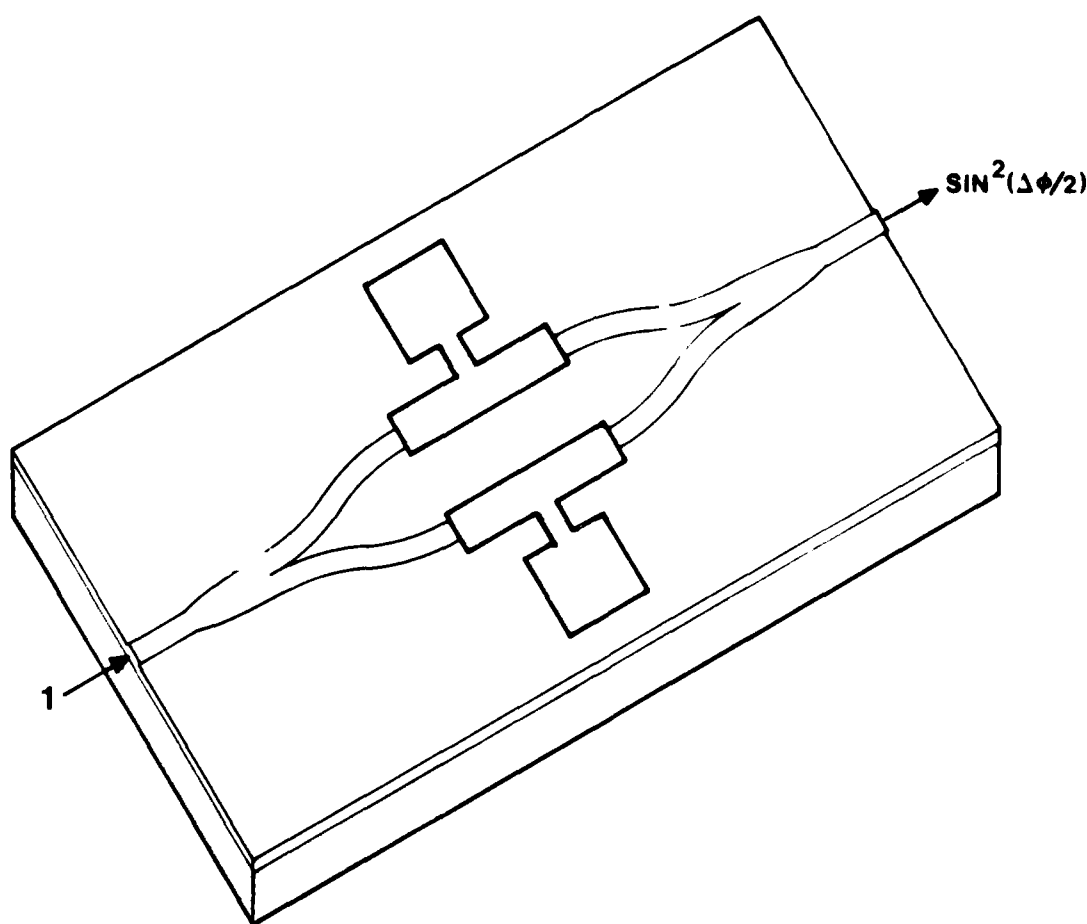


Figure 1-3. Mach-Zehnder Interferometric Switch. A voltage applied to the electrodes modulates the output channel. Since the output waveguide is single mode (no antisymmetric modes), any phase mismatched light is coupled to radiation modes.

One of the strengths of the thin-film ZnO on GaAs approach to optoelectronic circuits is that Schottky diode photodetectors can be easily fabricated in the GaAs substrate. Figure 1-5 depicts how light may be coupled from a waveguide to such a detector. Waveguide-to-detector coupling occurs through an opening in the buffer layer. Optimal coupling would require tapering of the buffer layer to prevent the back reflections which result from an abrupt discontinuity.

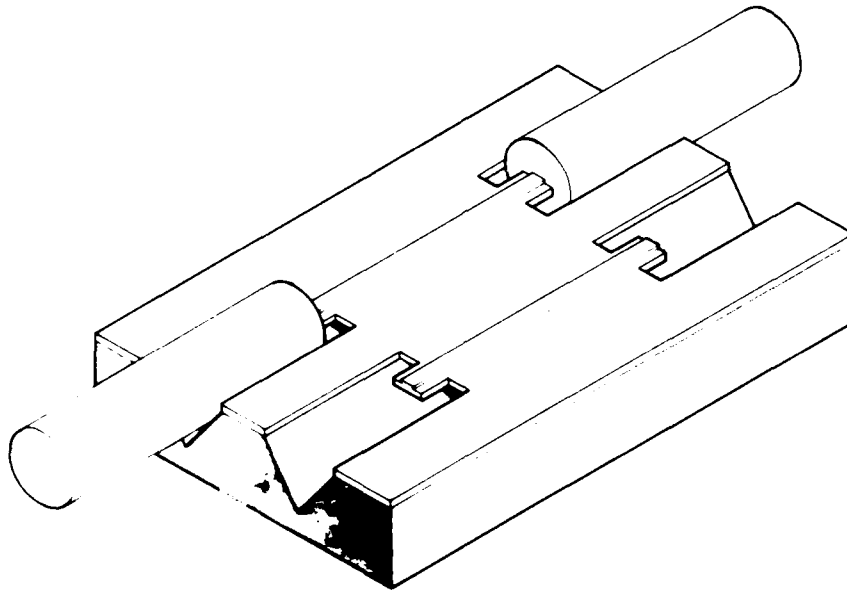


Figure 1-4. Fiber-to-Waveguide Coupling. Precision vee-grooves, anisotropically etched into the GaAs substrate, provide alignment of fibers to channel waveguides.

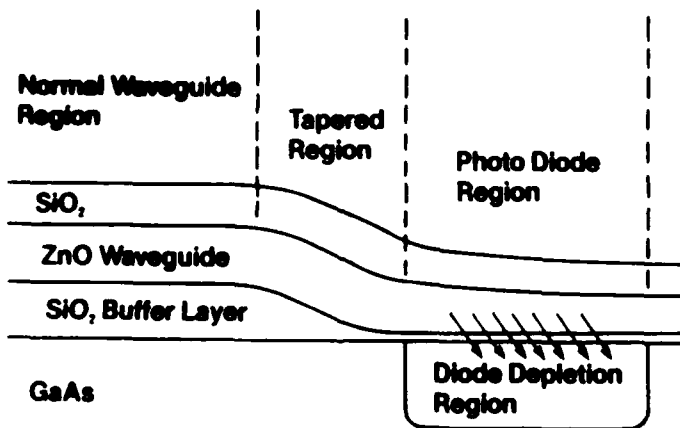


Figure 1-5. Integrated Waveguide Photodetector. An opening in the SiO₂ buffer layer causes light to be coupled to the high index GaAs substrate.

The foregoing discussion summarizes our approach to monolithic integration of waveguides, switches, couplers and detectors on a GaAs substrate. The emphasis throughout is on compatibility with mainstream GaAs electronics fabrication processes. Although optically passive devices may be realized using fiber-to-chip or laser-to-chip interconnects, the more useful devices will ultimately require monolithic integration of AlGaAs lasers. While laser integration is beyond the scope of this program, it remains a primary justification for selecting a GaAs substrate and a primary direction for future work.

The following sections will review the objectives, current status and future directions of the program.

Section II TECHNICAL OBJECTIVES

LONG-TERM OBJECTIVE

The long-term objective in pursuing the current research program is to develop monolithic optoelectronic circuits of thin-film zinc oxide on gallium arsenide (ZnO on GaAs) for optical signal processing applications.

Zinc oxide is a fairly unique waveguide material in that it can be sputter deposited at low temperatures to form well oriented poly crystalline films having very low optical losses and reasonably large piezoelectric and electrooptic effects.

OBJECTIVES OF CURRENT PROGRAM

The objective of the Thin-Film Optoelectronic Circuits Research Program is to identify and investigate IC-compatible fabrication processes for thin-film optoelectronic circuits of ZnO on GaAs. This technology will enable the monolithic integration of optical components with mainstream GaAs and Si microelectronics.

During the first year of the program, we have successfully met our objective of identifying and demonstrating IC-compatible fabrication methods for discrete optical components including waveguides, switches, detectors and fiber-to-waveguide couplers.

During this second year of the program, our objective is to integrate these various optical components into optical circuits on GaAs while still maintaining IC process compatibility. As a demonstration vehicle, we will fabricate 2 x 2 and 1 x 4 optical crossbar switches with fiber optic inputs and outputs.

Section III STATUS OF THE RESEARCH EFFORT

This section reports our efforts to develop IC-compatible fabrication processes for some basic thin-film optical components consisting of planar and channel waveguides, fiber-to-waveguide couplers, electro-optic switches, and integrated photodetectors. Our progress toward the Phase II goal of integrating these several processes is also reported. The section concludes with a summary of our accomplishments.

ZINC OXIDE MATERIAL

From the beginning, our efforts were hampered by difficulties in depositing ZnO films of suitable quality. This was primarily due to the vertical geometry of our RF sputtering system which gave a nonuniform film thickness and allowed "crumbs" of ZnO to rain down from the shutter and onto the substrate. The "crumb" problem was temporarily resolved at considerable effort by a thorough cleaning of the apparatus, but the situation was less than satisfactory. Because both this program and Honeywell's IR&D Optical Hybrid Gyro program require high quality ZnO films, we elected to undertake an internally funded effort to develop ion beam sputtered ZnO films. We had previously demonstrated that ion beam sputtering could produce high optical quality SiO₂, TiO₂ and Al₂O₃ films, but we had not used this technique for the deposition of ZnO. While developing the ZnO material, we have been able to substitute films of non-electrooptic Al₂O₃ for ZnO in many of our devices, but the demonstration of electro-optic switches has been unavoidably delayed.

We are now producing waveguiding films of ion beam sputtered ZnO. These films are of uniform thickness and quality over a 3-inch substrate. We expect that these films will continue to improve in quality and will impose no further delays to the Thin-Film Optoelectronic Circuits Program.

WAVEGUIDE STRUCTURES

One of the first problems to be resolved was the identification of a suitable buffer layer for isolating the optically guided wave from the lossy and higher index GaAs substrate. Adequate optical isolation requires a buffer layer thickness of about 1 micron. Sputtered oxides were unattractive because of their low deposition rates. In our previous work we had used thermally oxidized silicon substrates. This gave a high quality buffer layer but required several hours in a high temperature furnace, thereby violating our goal of compatibility with microelectronics. In any case, thermal oxidation is not possible with GaAs substrates.

We conducted a series of experiments to assess the quality of various SiO₂ films as buffer layers. We tested thermal SiO₂, ion beam sputtered SiO₂, and plasma deposited SiO₂. The plasma SiO₂ is most attractive in

that it can be deposited to considerable thicknesses quite rapidly. We deposited (or grew) 2 micron thick SiO₂ layers of each type on Si substrates. We then broke the wafers in half so we could deposit identical 1 micron thick waveguiding films of ion beam sputtered Al₂O₃ on each of the halves to be directly compared (two halves per deposition). We measured propagation loss of the TE₀₀ mode for each sample by using a pair of rutile coupling prisms and measuring optical throughput versus prism separation as the output prism was moved progressively closer to the input prism. To the ±0.5 dB/cm accuracy of the measurement technique, we observed no correlation of propagation loss with type of buffer layer. We therefore adopted plasma SiO₂ as both buffer and passivation layer for subsequent work.

Following the identification of plasma SiO₂ as a suitable buffer layer, our second major goal was to develop a process for fabricating the channel waveguide ridge structure as depicted in Figure 1-1.

A general characteristic of channel waveguides is some degree of excess scatter due to side wall roughness. A ridge waveguide structure has some inherent advantages in this respect. Since the ridge height is only 100-300 Å and the optical mode is confined predominantly beneath the ridge, scattering from the ridge sidewall should be much reduced. Our work prior to the program start had shown that a ridge of photolithographically deposited PMMA introduced little excess scatter. However, PMMA is quite hygroscopic and it would be difficult to find a sufficiently lower index material for a passivation layer. We therefore decided to form the ridge using a high index material, preferably the same material as the waveguiding film (ZnO).

Our baseline approach to ridge waveguide fabrication required etching the ZnO film everywhere except the ridge. It was a dismal failure. While virtually any etchant would attack the ZnO, our films were not uniform in their etch resistance, having both hard and soft spots on a fine scale. This is likely related to grain or column structure in these oriented polycrystalline films. Consequently, both the ridge sidewalls and the surrounding planar film were left in a very rough condition producing unacceptably high scatter.

Our revised approach was to deposit the ridge in a separate operation using a liftoff process. We initially used either Si₃N₄ or Al₂O₃ because they were more readily available than ZnO and the ridge was thin enough compared to the underlying ZnO film that a different ridge material was not expected to significantly perturb the electrooptic or piezoelectric properties of the overall structure. We found that some tearing of the ridge occurred during liftoff, giving a rather ragged sidewall in places.

Two further refinements brought us to our current fabrication process, depicted in Figure 3-1. First, a chlorobenzene soak was adopted to produce the overhanging photoresist structure shown in Figure 3-2. Following exposure, a 10 to 20 minute soak in chlorobenzene hardens the AZ-1350 photoresist to a depth dependent on the soaking time. During

development, the deeper lying photoresist then dissolves at a faster rate than near the surface, causing the observed undercutting. The overhanging photoresist then acts as a shadow mask for the subsequent ZnO ridge deposition, eliminating any tearing during liftoff. As an added benefit, the ridge sidewalls are more rounded perhaps, although this would be difficult to confirm. Figure 3-3 illustrates a typical waveguide ridge deposited by the overhanging resist liftoff process.

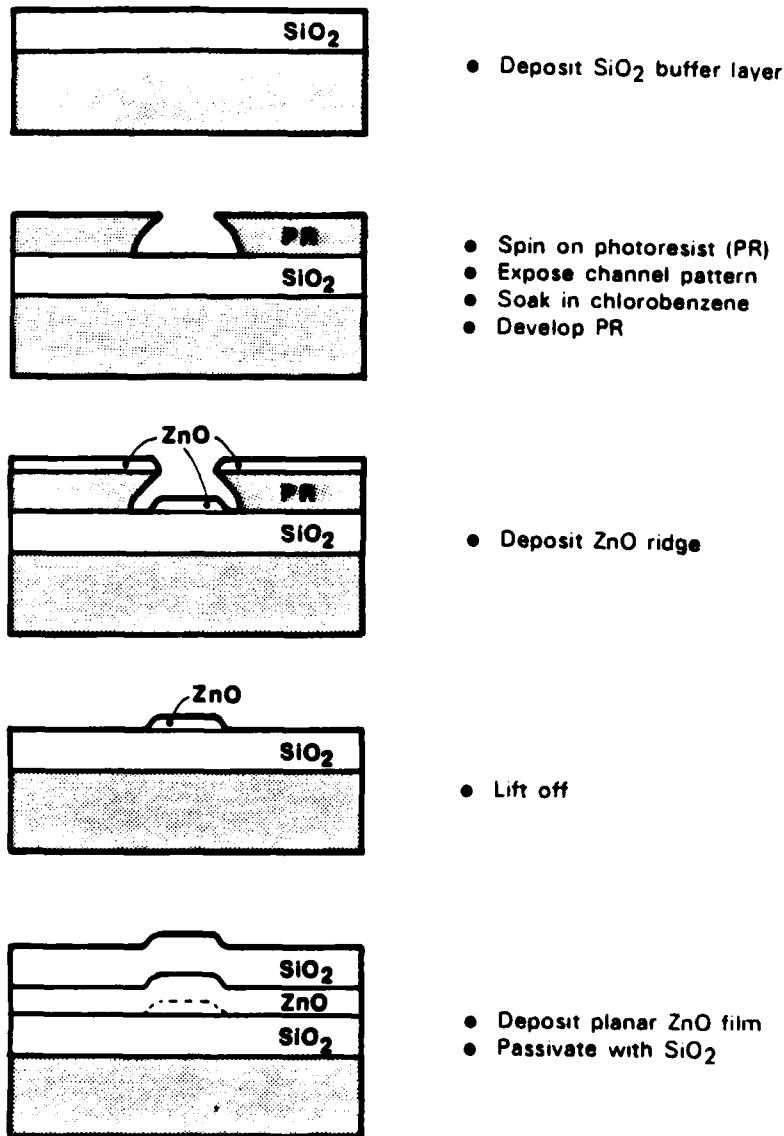


Figure 3-1. Channel Waveguide Fabrication Process. The overhanging photoresist shadow mask results in very smooth edges for the ZnO ridge. These edges are perhaps further smoothed by the planar ZnO deposition.

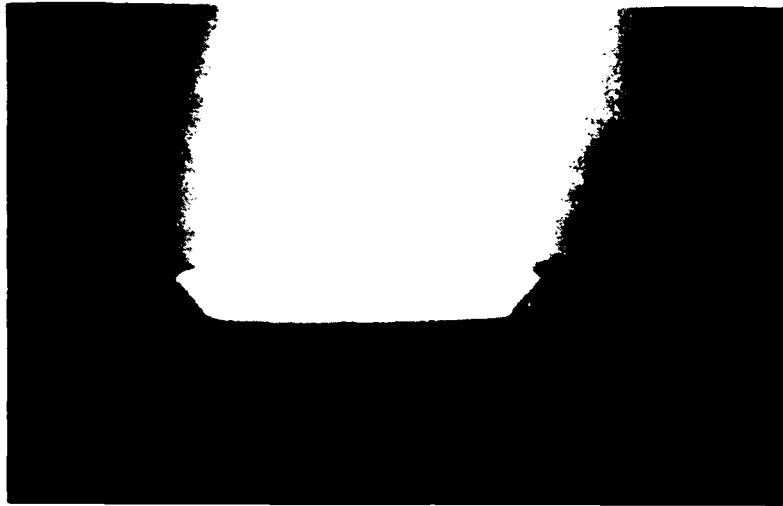


Figure 3-2. Photoresist Shadow Mask. The channel width is 3 microns.

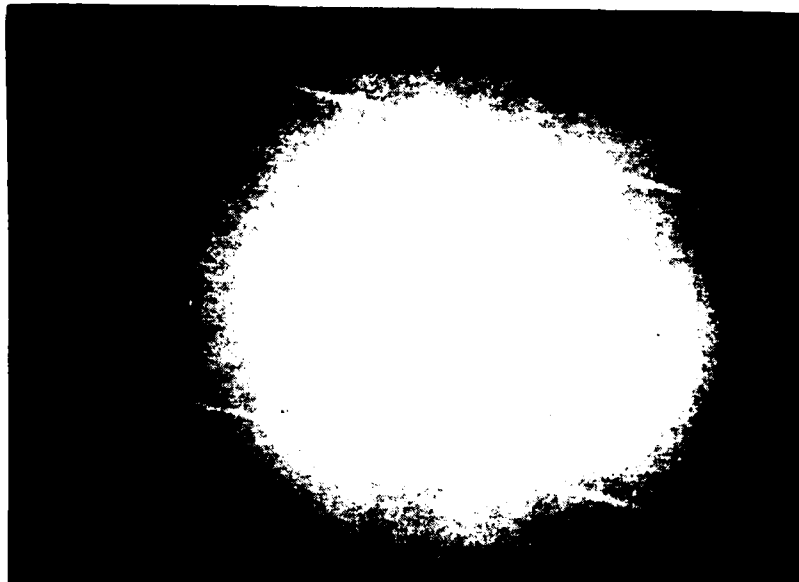


Figure 3-3. Waveguide Ridge. Three micron wide ridge of Al_2O_3 deposited on Si. Note the smooth side walls.

A final process refinement involves depositing the ridge prior to the planar film. This provides an opportunity for any residual roughness of the ridge sidewalls to be somewhat smoothed over during the subsequent planar deposition. Two additional benefits are that the more critical deposition occurs earlier in the process and ridge the height may be adjusted to compensate for photolithographic variations in channel width while still controlling the overall (ridge plus planar) thickness.

Figure 3-4 shows the calculated dependence of waveguide modes on ZnO film thickness for a planar waveguide. A buffer and passivation layer refractive index of 1.453 (SiO_2) and a wavelength of 8300 Å have been assumed. The ZnO films are birefringent with a refractive index near 1.9467 for TE modes and 1.9631 for TM modes. Cutoff of the second (TE_1) mode occurs at a film thickness of 3200 Å. In order to assure single mode operation, a film thickness near 3000 Å is chosen. This results in a vertical mode dimension of about 5600 Å for the TE_0 mode. The waveguide birefringence is due almost entirely to geometric effects.

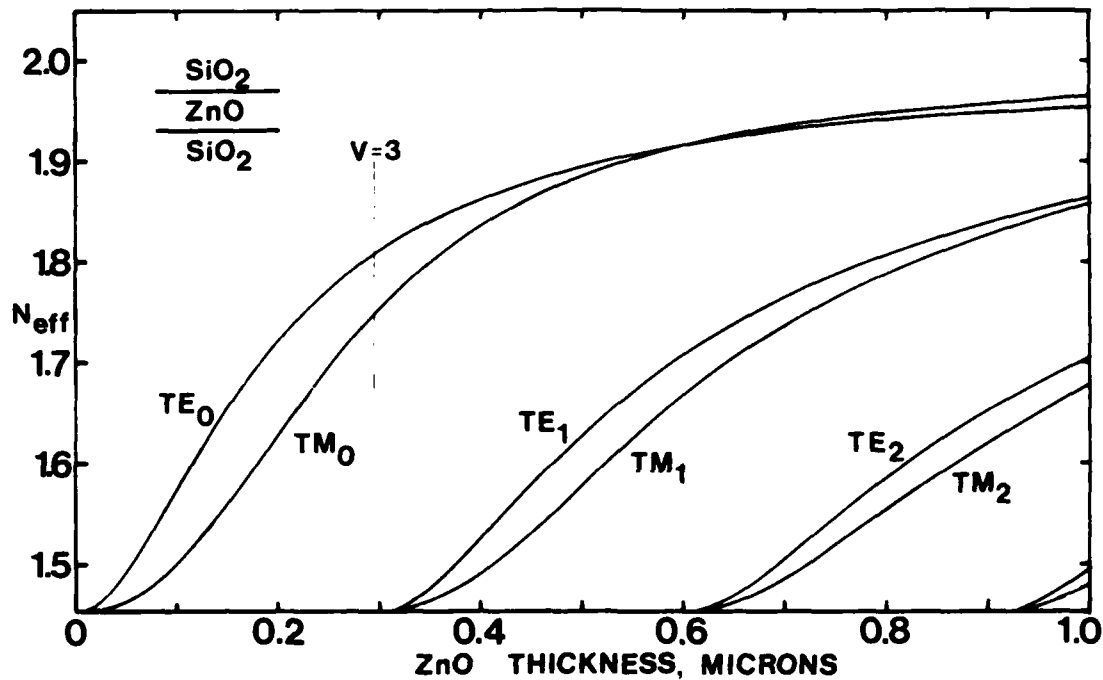


Figure 3-4. Modes of ZnO Thin-Film Waveguide. Single mode operation is achieved with a ZnO film thickness near 3000 Å.

The effective indices of deposited planar waveguides were measured using standard techniques of prism coupling with a pair of rutile prisms. A computer program was developed to solve for unknown waveguide parameters (e.g., film thickness) based on data from a number of waveguide modes. Meaningful solutions were obtainable with data from five or six modes, implying film thicknesses of 1 micron or more.

Our model for channel waveguides is based on the effective index approximation. Separate planar waveguide solutions are obtained for the ridge and for the surrounding field. The resulting modal indices are then used in solving an imaginary symmetric planar structure representing the waveguide in the lateral dimension. While this technique is somewhat lacking in rigor, it has been shown to yield

reasonable solutions so long as the ridge height is moderate and the mode is well confined. Numerical techniques would be required to obtain an exact solution.

Figure 3-5 indicates the dependence of ridge height on channel width for single-mode channel waveguides. Various combinations of ridge height and channel width will produce single mode guides. Therefore, ridge height can be varied to compensate for changes in wavelength, materials or processing. Curves are shown for waveguiding films of ZnO and Al₂O₃ and wavelengths of 8300 Å (AlGaAs) and 6328 Å (He-Ne). In all cases, buffer and passivation layers of SiO₂ have been assumed.

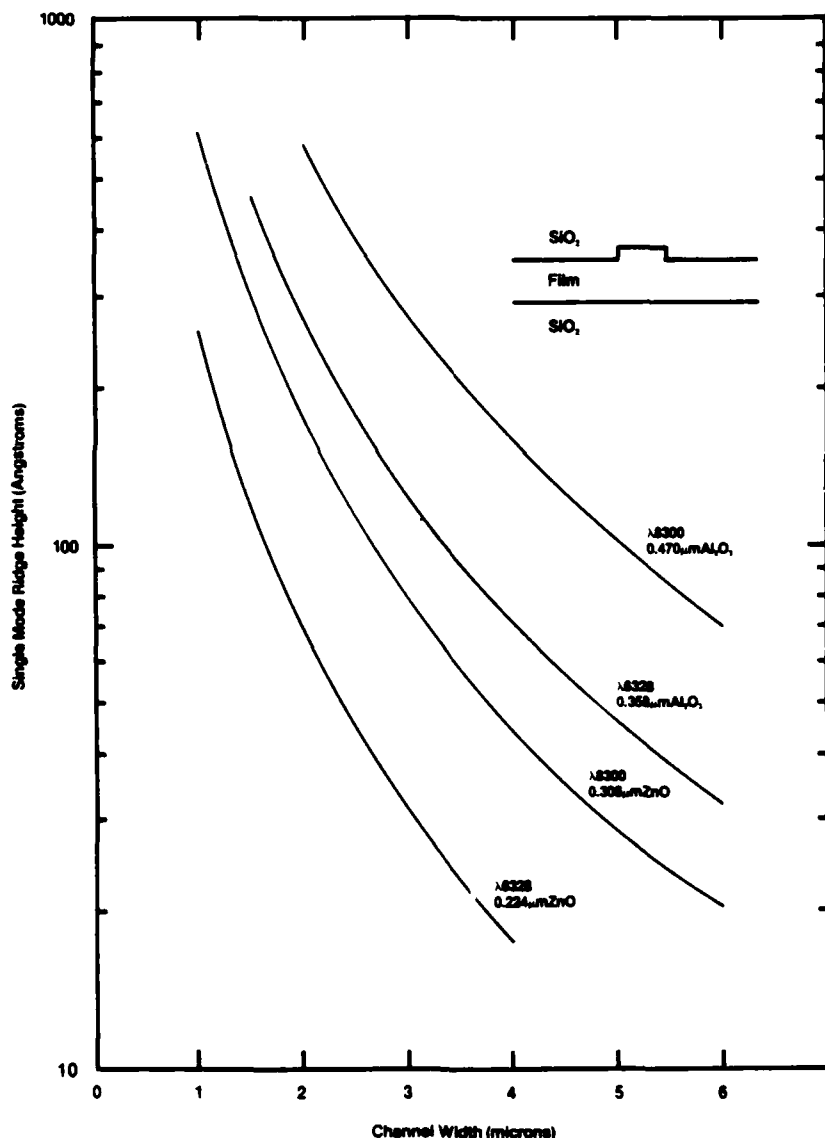


Figure 3-5. Dependence of Ridge Height on Channel Width. The curves are based on an effective index model.

The waveguide masks used in this first phase of the program were designed with channel widths of 2.5 microns which seemed to be a reasonable compromise between adequate lateral confinement and ease of fabrication. In fabricating these channel waveguides, we found that the channel width increased to 2.7 or 2.8 microns as a result of the various processing operations. It has therefore been our practice to measure channel width in the developed photoresist prior to depositing the waveguide ridges. This has permitted us to adjust ridge height as a means of compensating the increases in channel width. Our mask set for the second phase of the program is being designed with a channel width of 2.0 microns. This is expected to give an actual channel width close to our target of 2.5 microns.

Figure 3-6 is a computer plot of a two-level mask set used in fabricating thin-film waveguide components. Each of the 30 structures consists of a Y-branch waveguide of which one arm is a reference channel and the other an experiment. Experiments included 4-port directional couplers of various separations and interaction lengths, back-to-back tapers for measuring the losses due to tapering, and crossed channel structures to contain electro-optic grating switches. The metallization pattern (rectangles) is on the first mask level and helps in locating and identifying the channel waveguide experiments while also absorbing unwanted planar waveguide modes.

Figure 3-7 shows representative photos of the waveguide mask depicted in Figure 3-6. Mask photos are shown because the actual waveguides are nearly invisible and cannot be photographed. The Y-branch couplers consist of a parabolic tapered region which doubles the guide width, followed by a bifurcation region consisting of circular arcs. (All curved waveguides were formed using circular arcs of maximum possible radius in order to minimize bending losses.) The 4-port directional couplers consist of identical parallel waveguides plus curved sections to handle the offsets at each end. Coupling regions were 1 to 4 mm long with channel separations of 2 to 5 microns. Design parameters of the Y-branches, tapers and directional couplers were based on established mathematical models. Because no suitable model existed for the crossed channel waveguides, a correspondingly larger number of these devices was fabricated. Parabolic tapers were used to expand the crossed channels to widths varying from 2.5 (no taper) to 15 microns. The objective was to obtain a large enough crossing region for an efficient electrooptic diffraction grating without losing excessive light in the tapers. The angle of intersection was varied between 1.5 and 3.0 degrees, with larger angles expected to yield lower crosstalk at the expense of a shorter interaction region.

In Figure 3-8, a portion of a device, corresponding to the upper left corner of Figure 3-6, is shown just prior to the ridge deposition. The Y-branching waveguide channels show as dark lines in the photoresist liftoff mask. The metallic stops are positioned to absorb planar waveguide modes; only light guided by the channels will pass unattenuated through both sets of slots.

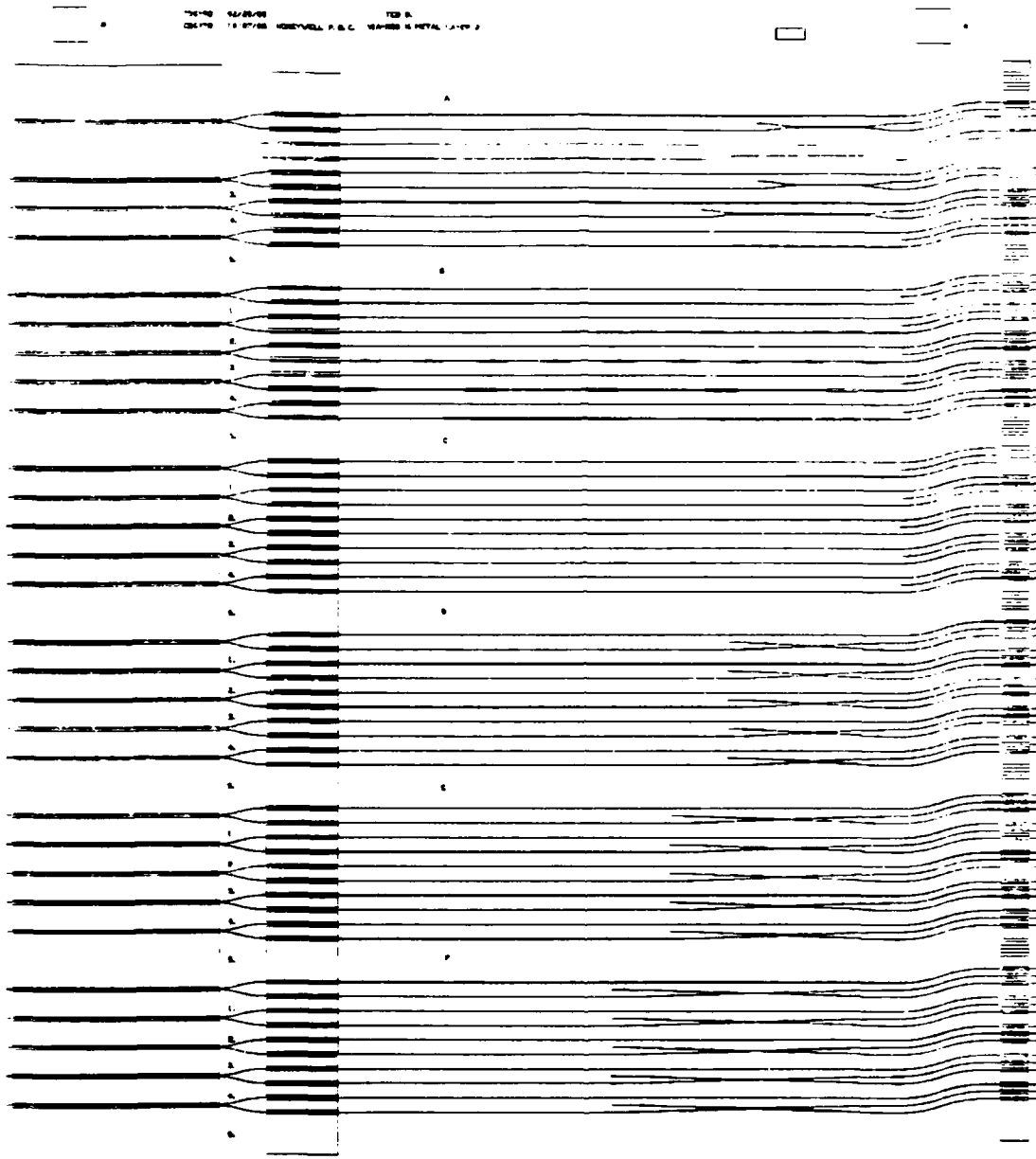


Figure 3-6. Computer Plot of Channel Waveguide Mask.
 Experiments include directional couplers (4),
 back-to-back tapers (9) and crossed channel
 structures (15).

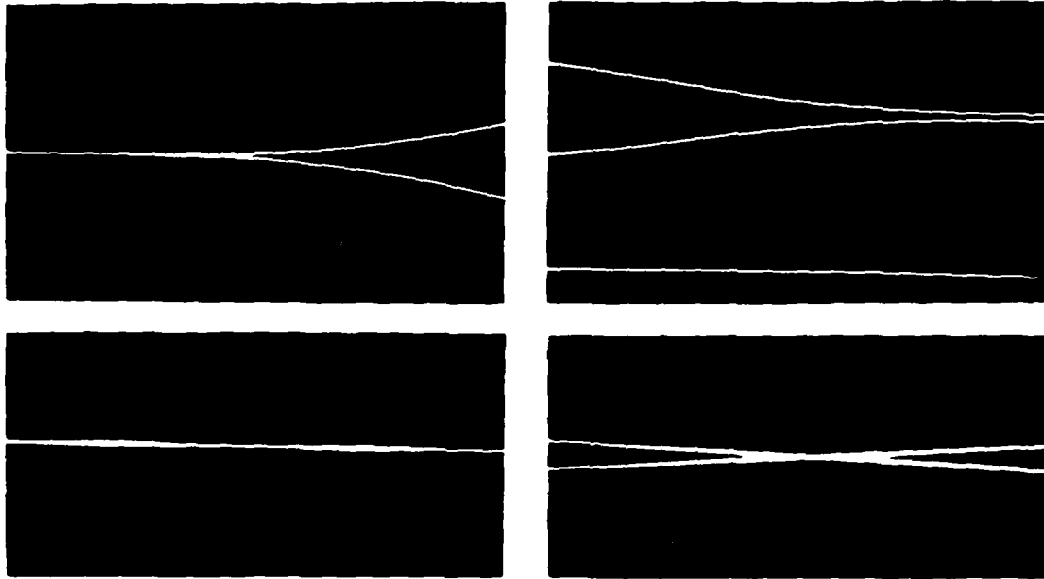


Figure 3-7. Photos of Channel Waveguide Mask. A Y-branch coupler, part of a directional coupler, back-to-back tapers and a crossed channel structure are pictured.

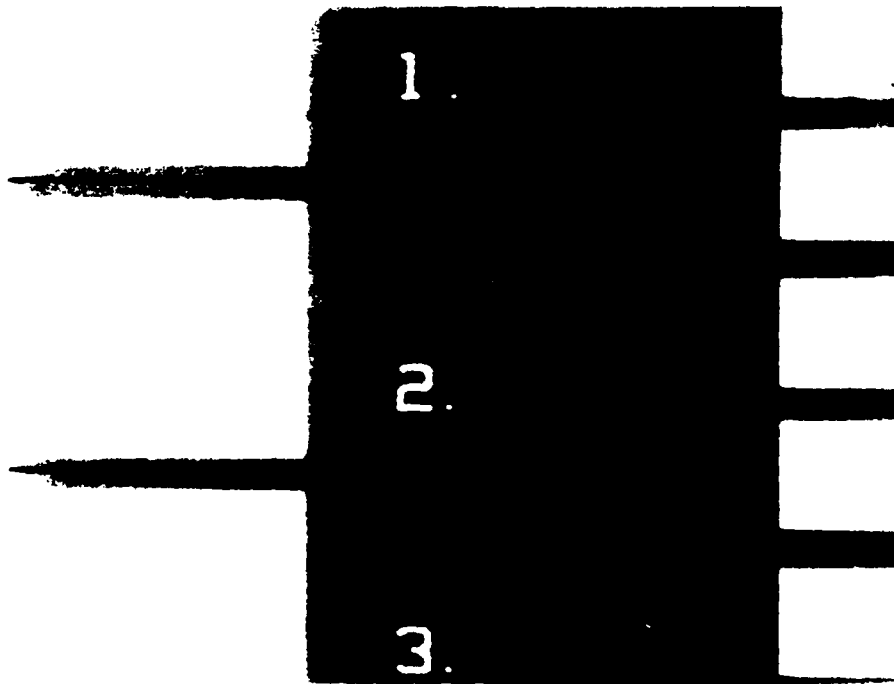


Figure 3-8. Thin-Film Channel Waveguides. A portion of a device is shown ready for the ridge deposition.

All testing of channel waveguide devices was performed using the evaluation facility depicted in Figure 3-9. The optics are optimized for use at the AlGaAs diode laser wavelength of 830 nm. A co-propagating HeNe laser (633 nm) is also available for preliminary measurements and system alignment. Separate sample stations are provided for testing of planar and channel waveguides. The prism coupling station is used for measuring modal indices and propagation losses of planar films. The end-fire coupling station is provided for routine testing of channel waveguide devices. Output channels of the device are imaged to an IR vidicon for examination of near-field modal patterns. The end-fire station also includes a stereo zoom microscope for top-down examination of the sample surface. In this manner, channel waveguides are observed via their scattered light.

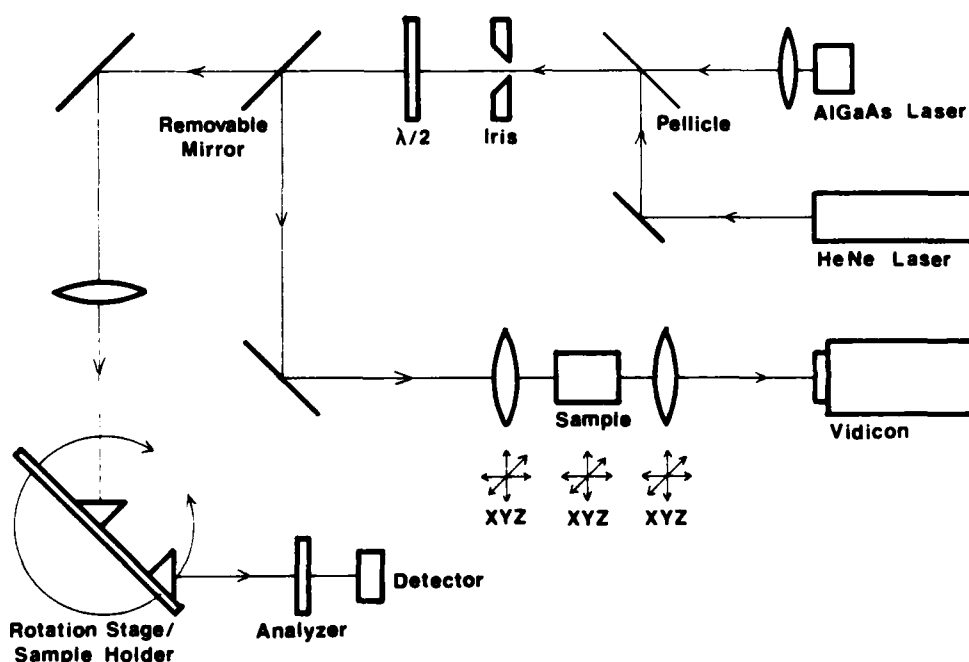


Figure 3-9. Waveguide Evaluation Facility. Fixturing is included for both end-fire and prism coupling to thin-film waveguides.

FIBER-TO-WAVEGUIDE COUPLING

Initially, fiber-to-fiber coupling tests were used to determine the suitability of etched vee-grooves for fiber alignment. Single-mode fibers having a 125 micron cladding diameter and a 5 micron core diameter were butt-coupled using silicon vee-grooves for alignment. Coupling efficiencies of 80 percent and better were routinely obtained. Coupling efficiency showed little dependence on axial rotation, indicating that concentricity of fiber core and cladding would not be a significant problem.

We found that fiber-to-fiber vee-groove splices could be made permanent by cementing with UV curing epoxy. As a side benefit, the index matching properties of the epoxy led to improved coupling efficiency. To solve a problem of excess epoxy contaminating adjacent vee-grooves, a technique was developed whereby the cleaved fiber end was dipped in epoxy and then wiped almost clean prior to insertion in the vee-groove. We have found that a slight pressure is required to seat an epoxied fiber in a vee-groove and that this pressure can be varied somewhat to fine tune the coupling. This provides a means of compensating variations in fiber diameter and groove depth.

Our approach to fabricating the fiber-to-waveguide coupler of Figure 1-4 involves opening channels in the deposited $\text{SiO}_2\text{-ZnO-SiO}_2$ waveguide structure and using the oxide layers as an etch mask for the anisotropic vee-groove etch. Because of the difficulty of doing photolithography on significantly nonplanar substrates, this vee-groove etch should be the final step in the fabrication process. A LAM (plasma) etcher is used for making quite vertical cuts through the oxides, stopping at the GaAs substrate.

Ideally, the depth of vee-grooves would be limited by the boundaries of the LAM-etched slots in the oxide and by 111 crystallographic planes of the GaAs substrate. To align the core of a 125 micron diameter fiber to a thin-film waveguide requires a groove width of 150 to 152 microns, depending on the buffer layer thickness. A longer etching time should produce a deeper but not a wider vee-groove. Silicon etchants are close to this ideal and the precision with which vee-grooves can be etched into 100 silicon exceeds typical variations in fiber diameter. GaAs etchants, on the other hand, are not nearly as directional and significant undercutting of the oxide mask occurs. Up to 12 microns or so of undercutting can be compensated by making a narrower slot in the oxide, but the slot must be wide enough to admit the fiber diameter. Therefore the rate of undercutting must be less than about 20 percent of the vertical (i.e., 100) etch rate.

A number of GaAs etchants were tested in an attempt to find one that would be sufficiently anisotropic. Our best results have been obtained with acidic hydrogen peroxide etchants. These have consisted of varying concentrations of $\text{H}_2\text{SO}_4\text{:H}_2\text{O}_2\text{:H}_2\text{O}$, $\text{H}_3\text{PO}_4\text{:H}_2\text{O}_2\text{:H}_2\text{O}$ or $\text{HCl:H}_2\text{O}_2\text{:H}_2\text{O}$. We have also tried mixtures of $\text{NH}_4\text{OH:H}_2\text{O}_2\text{:H}_2\text{O}$. We continue to investigate various GaAs etchants as a means achieving better control over vee-groove depth.

Another aspect of fiber-to-waveguide coupling is mode matching. In contrast to Ti:LiNbO_3 waveguides, our thin-film waveguides are well matched to diode lasers but poorly matched to fibers. The mode dimensions of our single mode thin-film waveguides are about 4.6 microns horizontal by 0.6 microns vertical. Typical single mode fibers have mode diameters of 5 to 6 microns. Simple butt coupling of fiber to waveguide results in losses of 9 to 11 dB due almost entirely to the difference in vertical mode dimension.

There are a number of possible approaches to improving vertical mode matching. We had originally proposed using an optical fiber in a transverse vee-groove as a cylindrical lens, overlooking the fact that transverse grooves in GaAs have dovetail profiles. A better approach is to increase the vertical mode dimension of the thin-film waveguide by reducing the thickness of the waveguiding film.

Figure 3-10 shows the dependence of mode dimension on film thickness for a symmetric $\text{SiO}_2\text{-ZnO-SiO}_2$ structure. Figure 3-11 depicts how film tapering could be used to achieve fiber-to-waveguide mode matching. Our baseline film thickness of 3000 \AA was selected in order to achieve low-loss single-mode operation. Much thinner films will result in a significantly increased mode dimension. The exact location and rate of the tapering are not critical. A more gradual transition will reduce mode conversion losses but a longer propagation distance at the larger mode dimension will result in greater losses to the substrate.

We propose to demonstrate the structure of Figure 3-11 during this current phase of the program. A film thickness of about 100 \AA , equal to the waveguide ridge height, should result in a vertical mode dimension of 4 microns, about the same as the mode diameter of an optical fiber. We will first deposit the 100 \AA ridge and then use a mechanical shadow mask to taper the subsequent planar ZnO deposition to zero in the vicinity of the vee-grooves. The tapering will have the additional benefit of reducing the effective refractive index of the waveguide, thus reducing Fresnel reflections. Overall, the coupling loss should be reduced from an initial 9-11 dB to perhaps 3 dB.

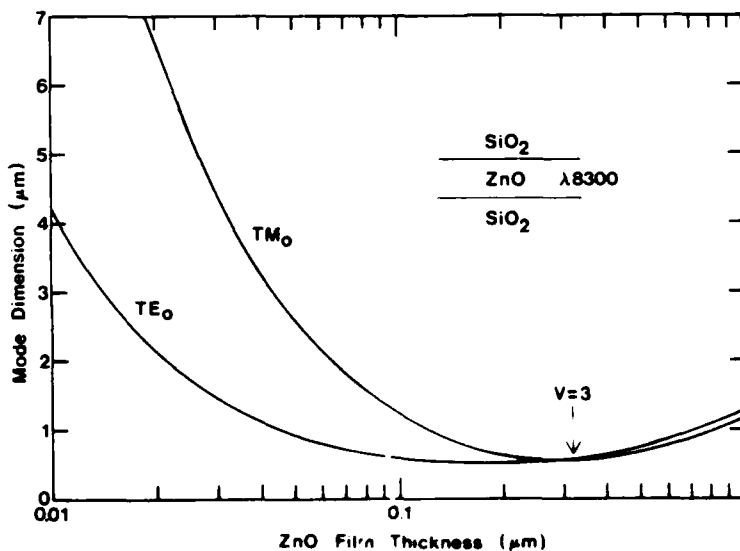


Figure 3-10. Dependence of Mode Dimension on ZnO Film Thickness. The most effective (and easiest) method of increasing the optical mode dimension is to decrease the ZnO film thickness.

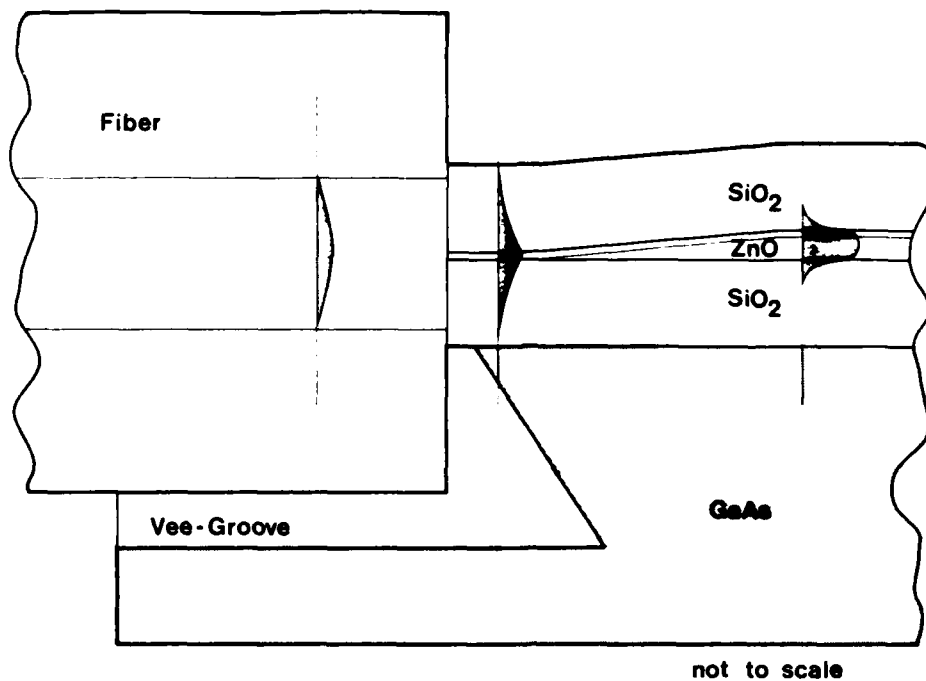


Figure 3-11. Fiber-to-Waveguide Mode Matching. The shaded areas represent the optical mode profile at three dissimilar points along the path. Tapering the ZnO film thickness enlarges the waveguide mode dimension to better match that of the fiber.

ELECTRO-OPTIC SWITCHES AND MODULATORS

Electro-optic devices are key components in many integrated optic circuits. Sputtered ZnO is polycrystalline with its c-axis oriented vertically but orthogonal axes oriented randomly in the plane. Thus, only vertical field components contribute to an electro-optic effect. The relevant electro-optic coefficients are $r_{13} = -1.4 \times 10^{-12}$ m/V for TE modes and $r_{33} = +2.6 \times 10^{-12}$ m/V for TM modes. Vertical fields can be most efficiently produced by placing electrodes both above and below the ZnO film. Despite the smaller r_{13} coefficient, TE mode devices are to be preferred because of the strong attenuation of TM modes by the electrode structure. Uncompensated zinc oxide films are semiconducting with an average breakdown voltage $E_{\max} = 8 \times 10^6$ V/m. Therefore, the maximum electro-optically induced refractive index change will be less than $\Delta n = -n^3 r E_{\max} / 2 = +4 \times 10^{-5}$. For electro-optic devices requiring a $\pm \pi/2$ phase shift, electrical breakdown dictates a minimum device length of 5 mm, roughly twice the length of comparable LiNbO₃ devices. There is, however, a significant difference. The length of a LiNbO₃ electro-optic device is typically limited by the need for a reasonable drive voltage (50-100 V), whereas thin-film ZnO devices can operate at much lower drive voltages (8-12 V) because their vertical electrode structure typically results in a narrower electrode gap.

Because of our substitution of nonelectro-optic Al_2O_3 for ZnO , we have thus far been unable to test any electro-optic switches. We have, however, fabricated several relevant waveguide structures such as Y-branches and directional couplers. Now that we are producing ZnO films by ion-beam sputtering, we fully intend to demonstrate thin-film electro-optic switches of both the directional coupler and Mach-Zehnder types. The directional coupler switches (Figure 1-2) have been designed with an electrode length of 3 mm. This somewhat less than the calculated minimum length based on average breakdown voltage. We felt, however, that the benefits of demonstrating shorter devices outweighed the risk of not being able to fully modulate them. Since the ZnO breakdown voltage is reported to vary from 5×10^6 to at least 20×10^6 V/m, it seems likely that at least some of our devices will be fully functional. The required drive signals will be in the vicinity of 20 volts. If successful, we will have demonstrated that thin-film ZnO electro-optic devices can be as short as and have lower drive voltages than their LiNbO_3 counterparts.

INTEGRATED PHOTODETECTORS

Our design for an integrated waveguide photodetector is depicted in Figure 3-12. The electrodes extend through an opening in the SiO_2 buffer layer to form Schottky contacts to the semi-insulating GaAs substrate. Depending on the doping concentration, a bias voltage of 20 to 50 volts will extend the diode depletion region fully across the 8-micron inter-electrode gap. As light is coupled from the channel waveguide to the higher index GaAs, photocarriers are generated in the inter-electrode gap. Up to the breakdown voltage of the GaAs, photocurrent should increase monotonically with increasing bias. In Figure 3-12, the additional metallization surrounds the detector to absorb any stray light guided in planar modes.

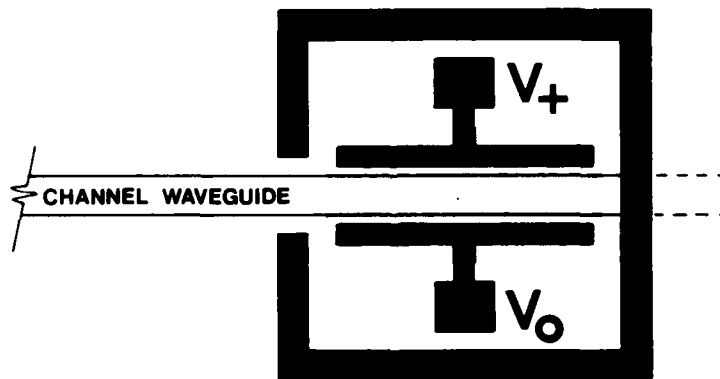
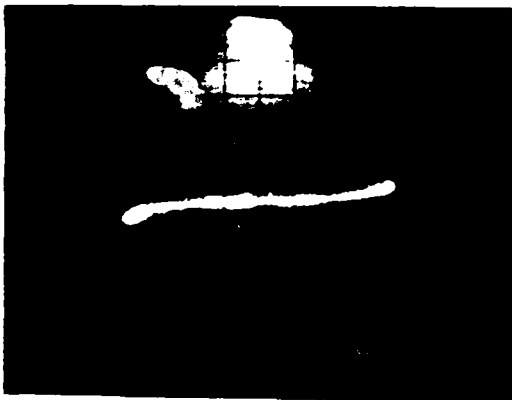


Figure 3-12. Integrated Photodetector for Channel Waveguides. An opening in the SiO_2 buffer layer causes light to be coupled from the ZnO waveguide to the higher index GaAs substrate. Back-to-back Schottky diodes form a simple but effective photodetector.

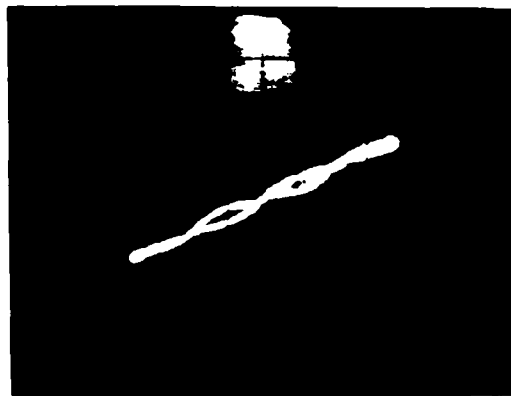
Initially, our intent had been to use an interdigitated electrode pattern in order to obtain both a large enough detector area and a sufficiently small inter-electrode gap. Interdigitated electrode patterns have the disadvantage that a portion of the incident light is blocked by the electrodes. The Schottky photodetector concept was tested and the permissible inter-electrode gap determined by fabricating interdigitated Ti-Au electrode patterns on a GaAs substrate. These periodic structures had equal width electrodes and gaps of 4, 6 or 8 microns. They were tested with illumination incident normal to the surface. Representative I-V curves with and without illumination are shown in Figure 3-13. The somewhat low breakdown voltage of 20 volts is likely attributable to the use of Ti-Au as the electrode metallization. A barrier metal (e.g. Ti-Pd-Au or Ti-Mo-Au) would prevent diffusion of the gold into the GaAs.

After determining that the inter-electrode gap could be as wide as 8 microns, we adopted the parallel electrode geometry of Figure 3-12. With this geometry, we expect virtually no absorption of light by the electrode structure. In fact we anticipate that, by optionally omitting the buffer layer openings, we will make the detectors invisible to the optical guided waves. This may prove a most useful option when testing the other waveguide devices.

The maximum useful electrode length for the integrated waveguide photodetector is dependent on the distance required to couple light from the waveguiding film to the GaAs substrate and also on the amount of scattering or spreading occurring when the optical guided wave encounters the buffer layer opening. Excessive electrode length (or width) will result in larger dark current and capacitance. We will test detectors with buffer layer openings varying in length from 50 to 300 microns.



ROOM LIGHTS ONLY



MICROSCOPE ILLUMINATOR ON

Figure 3-13. I-V Characteristic of Back-to-Back Schottky Photodetector. The scales are 50 volts per horizontal division and 5 μ A per vertical division.

PROCESS INTEGRATION

In the course of fabricating the various discrete waveguide components demonstrated during the first year of the Thin-Film Optoelectronic Circuits Research Program, we have developed a number of specialized fabrication processes. During this second year of the program, our primary objective is to integrate these separate processes into a single overall process which will be used to fabricate complete optical circuits on a single substrate.

Our baseline fabrication process, summarized in Figure 3-14 and described in the following paragraphs, has served as a framework for the design and layout of a mask set for the Phase II optical circuit demonstration. CALMA plots of this mask set are included herein as an Appendix. The optical circuits fabricated by this process will have an electro-optically active GaAs-SiO₂-ZnO-SiO₂ waveguiding structure with electrodes above and below the ZnO waveguiding film. The GaAs substrate will have Schottky photodiodes and vee-grooves for the alignment of optical fibers. In keeping with the program objectives, the baseline process is fully compatible with mainstream GaAs IC fabrication and can potentially accommodate a large variety of active electro-optic and acousto-optic devices.

The fabrication process begins with the plasma deposition of an SiO₂ buffer layer to isolate the optical field from the lossy GaAs substrate. If GaAs Schottky photodiodes are to be used, apertures are then etched through this buffer layer to allow coupling between waveguides and detectors. Next, a first metallization layer is patterned to form the Schottky contacts, shunting electrodes for the electro-optic and acousto-optic devices, and also various alignment and identification marks. If waveguides are to pass directly over this first metallization (e.g., electro-optic switches), then a second, thin (1500-2000 Å) SiO₂ buffer layer is deposited. This layer functions to prevent optical attenuation by the metal electrodes while still allowing efficient waveguide-to-detector coupling.

The next step in the fabrication process is deposition of ZnO channel waveguides using the two-step ridge and planar depositions as described previously. This is followed by another thin SiO₂ buffer layer, the upper electrode metallization, and a thicker SiO₂ passivation layer.

Electrical contacts to the device are established by etching through the oxide layers to the underlying bonding pads and then depositing additional gold by a liftoff process. During the same operation, optical stops are etched through selected portions of the SiO₂-ZnO-SiO₂ structure to prevent unwanted planar waveguide modes.

The final processing step is the etching of vee-grooves for the attachment of optical fibers. Vee-groove delineation is necessarily the last photolithography step because the deeply etched vee-grooves make subsequent spin coating of photoresist extremely difficult. This step is omitted if the device is to be tested by end-fire coupling methods.

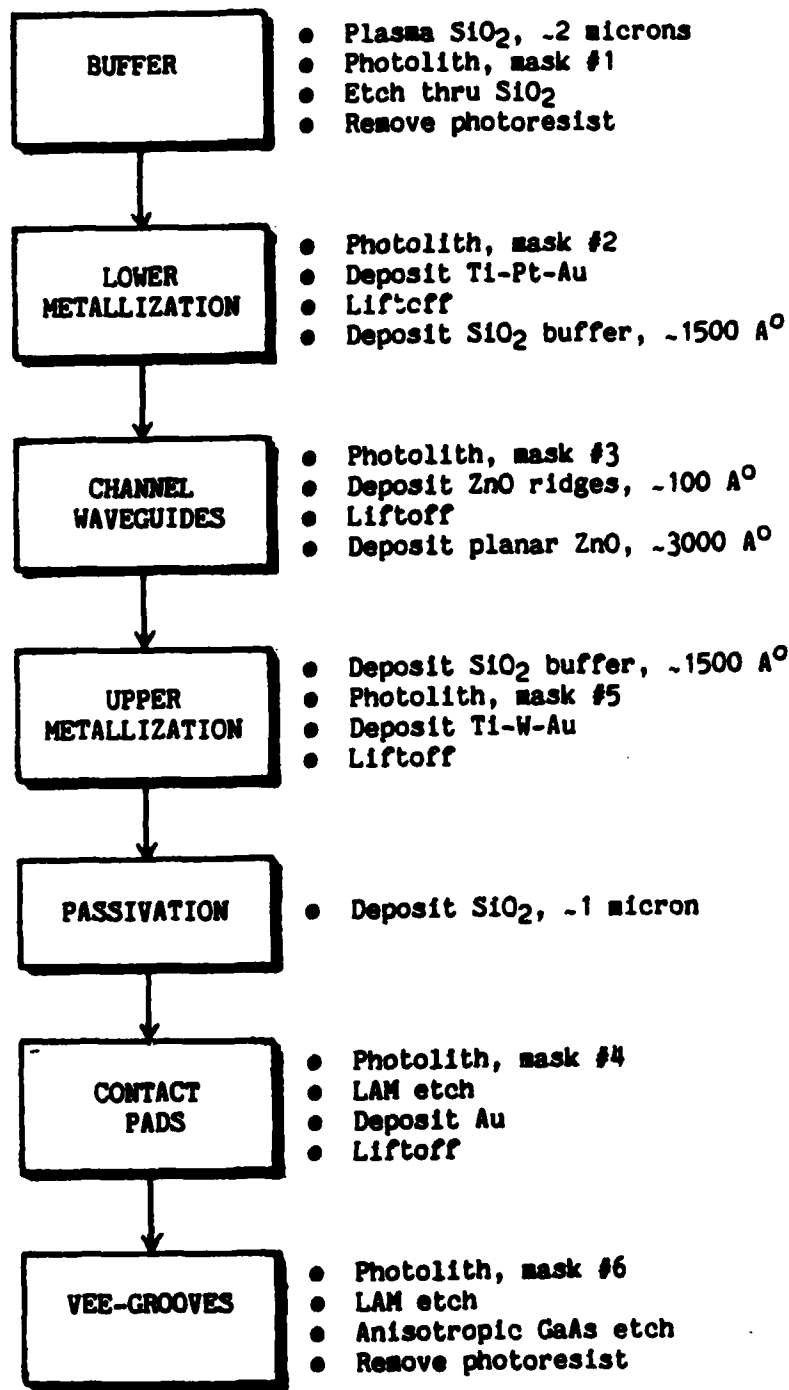


Figure 3-14. Optical Circuit Fabrication Process. This process is fully compatible with mainstream GaAs IC fabrication and can potentially accommodate a large variety of active electro-optic and acousto-optic devices.

SUMMARY OF ACCOMPLISHMENTS

The overall objective of the Thin-Film Optoelectronic Circuits Research Program has been to identify and investigate IC-compatible fabrication processes for thin-film optoelectronic circuits of ZnO on GaAs. This technology will enable the monolithic integration of optical components with mainstream GaAs and Si microelectronics. Our major accomplishments in support of this objective are as follows:

- Established the suitability of plasma deposited SiO₂ as a low index buffer layer for thin-film waveguide structures fabricated on GaAs.
- Developed and demonstrated an innovative and versatile ridge deposition technique for fabricating thin-film channel waveguides having little excess loss due to sidewall scattering.
- Fabricated and tested a variety of channel waveguide bends, tapers, Y-couplers, directional couplers, and crossovers.
- Developed a GaAs vee-groove etching technique and demonstrated fiber-to-fiber alignment with coupling efficiencies of better than 80 percent. Developed a method of permanently mounting fibers in vee-grooves.
- Designed efficient thin-film ZnO electro-optic switches which we expect to operate at lower drive voltages than LiNbO₃ switches of comparable length.
- Developed a novel concept for monolithically integrated channel waveguide Schottky photodetectors and demonstrated feasibility.
- Developed an IC-compatible baseline fabrication process for thin-film optoelectronic circuits on GaAs.
- Completed the design and mask layout for a thin-film optoelectronic circuit demonstration. This device, which will be fabricated and tested during this current program phase, includes 1 x 4 and 2 x 2 optical crossbar networks, Mach-Zehnder interferometric waveguide modulators, integrated GaAs photodetectors, and vee-groove aligned fiber optic pigtails.

Section IV FUTURE PLAN OF THE PROGRAM

During the first year of the Thin-Film Optoelectronic Circuits Research Program, we successfully identified and demonstrated IC-compatible fabrication methods for several discrete optical components. Our objective during this second year of the program is to integrate these various optical components into a single optical circuit on GaAs while still maintaining IC process compatibility. As a demonstration vehicle, we will fabricate 2 x 2 and 1 x 4 optical crossbar switches with fiber optic inputs and integrated photodetector outputs. We have already made significant progress toward accomplishing this objective. The program schedule and statement of work are described below.

PROGRAM SCHEDULE

The Phase II program schedule (Figure 4-1) includes the four major tasks of (1) process integration, (2) optical circuit design and layout, (3) optical circuit fabrication and (4) optical circuit testing and evaluation. Note that the schedule is for February 1986 through January 1987. The shaded regions indicate progress to date.

STATEMENT OF WORK

The following statement of work describes the specific tasks to be performed under Phase II of the Thin-Film Optoelectronic Circuits Research Program.

Task 2.1 -- Process Integration

We will integrate the fabrication processes for the various optical components into a single, comprehensive process for fabricating all optical components on a single substrate. Incompatibilities in the component processes will be resolved while maintaining full compatibility with mainstream GaAs IC fabrication processes.

We have made substantial progress toward completion of this task, resulting in a baseline fabrication process as presented in Figure 3-14. Additional work will be required to perfect and document the process.

Task 2.2 -- Optical Circuit Design and Layout

This task, which has now been completed, involves the device design and mask layout for a thin-film optical circuit having waveguides, fiber-to-waveguide couplers, electro-optic switches, and detectors. CALMA plots of the individual mask levels are included as an Appendix. The optical circuit selected for demonstration includes 2 x 2 and 1 x 4 optical crossbar switches.

**THIN FILM
OPTOELECTRONIC CIRCUITS
RESEARCH PROGRAM**

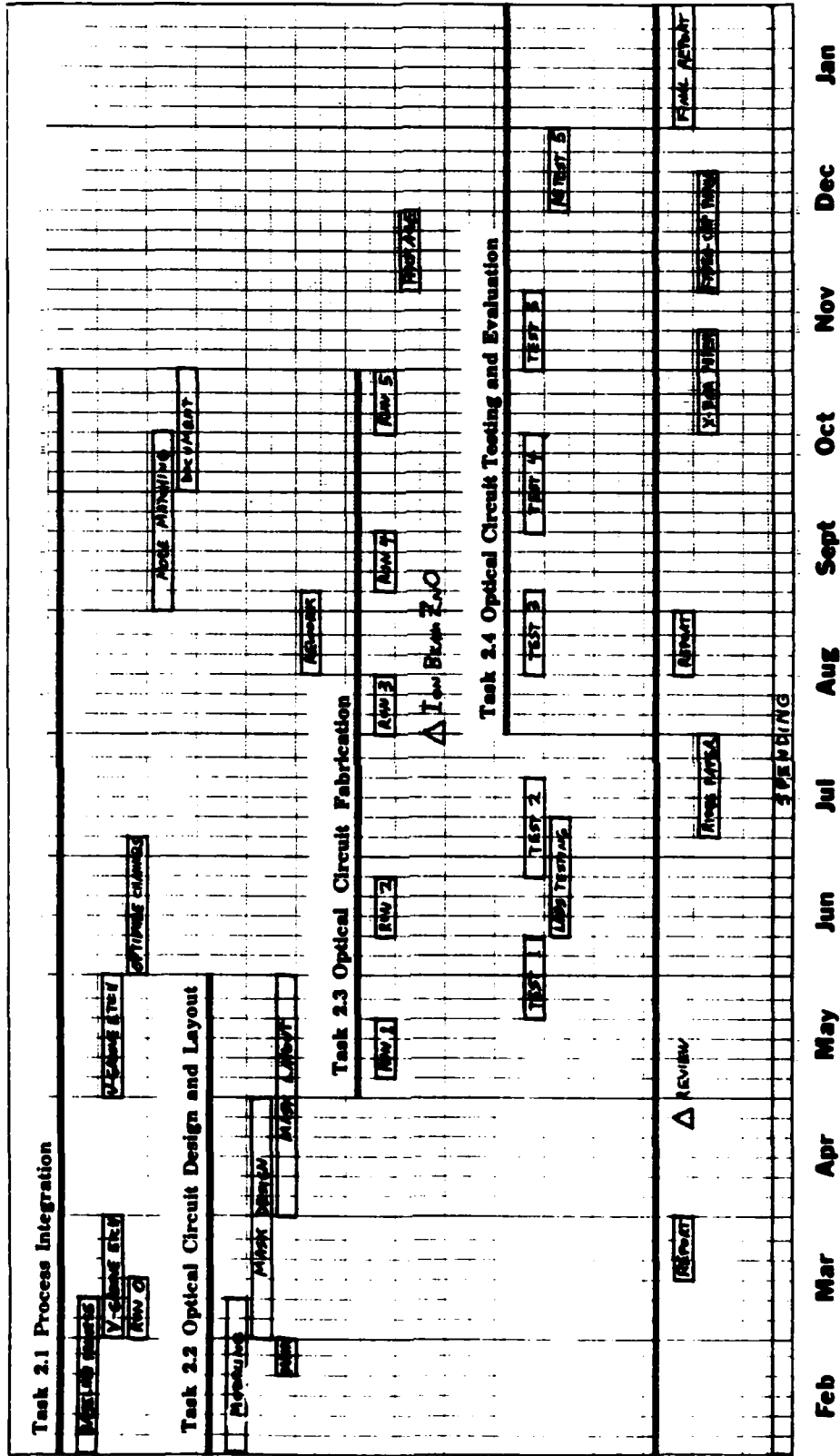


Figure 4-1. Phase II Program Schedule.

Task 2.3 -- Optical Circuit Fabrication

The optical circuit designed in the previous task will serve as a vehicle for demonstrating and perfecting the fabrication process. The mask set has been designed to allow a high degree of flexibility. For example, both the vee-groove and the detector aperture fabrication steps can be omitted if the waveguide devices are to be tested by end-fire coupling methods. This will permit more rapid iteration of fabrication and testing.

As described in Section III, early difficulties with RF sputtering of ZnO films led us to initiate an internally funded effort to develop ion beam sputtered ZnO films while temporarily substituting films of ion beam sputtered Al₂O₃ in our passive waveguide devices. The substitution of Al₂O₃ for ZnO requires only minor modification of the fabrication process (a change of film thickness), but the resulting devices are not electro-optically active. We are now producing ZnO films by ion beam sputtering and plan to incorporate these films into our devices beginning in August.

To reduce the risk of changing from Al₂O₃ to ZnO waveguides, we have planned a series of five processing runs, summarized in Table 4-1. The first two runs use the now familiar Al₂O₃ passive waveguides to test more confidently the process integration including, in the second run, fiber-to-waveguide and waveguide-to-detector coupling. The third run, introducing ion beam sputtered ZnO, will again use end-fire coupling to demonstrate more quickly electro-optically active ZnO devices. The fourth run will include full integration of all devices in ZnO. If time and resources permit, a fifth and final run will seek to demonstrate tapering of the ZnO film for improved fiber-to-waveguide mode matching.

Table 4-1. Phase II Processing Runs

RUN	FILM	INPUT	DEVICE	OUTPUT
1	Al ₂ O ₃	End-Fire	Passive Guides	Cleaved
2	Al ₂ O ₃	Fibers	Passive Guides	Some Detectors
3	ZnO	End-Fire	Active Switches	Cleaved
4	ZnO	Fibers	Active Switches	Fibers, Detectors
5	ZnO	M. M. Fibers	Active Switches	Fibers, Detectors

Task 2.4 -- Optical Circuit Testing and Evaluation

The goal of this task will be to verify that the various optical components perform as designed when integrated into monolithic optical circuit. The bulk of the device testing will be performed using

end-fire coupling. Selected devices will be fiber-pigtailed and packaged for high speed testing. Parameters to be measured include modal properties and attenuation losses of waveguides, voltage switching characteristics, cross talk and insertion loss of directional coupler and Mach-Zehnder switches, responsivity of integrated photodetectors, and insertion loss of fiber-to-waveguide couplers.

DIRECTIONS FOR FUTURE RESEARCH

Upon successful completion of Phase II of the Thin-Film Optoelectronic Circuits Research Program, we will have demonstrated IC compatible fabrication of several thin-film integrated optic devices on GaAs substrates. When compared to AlGaAs devices on GaAs, our thin-film waveguide devices are expected to exhibit the advantages of lower attenuation loss and greater ease of fabrication. Although we will not have explicitly demonstrated the integration of optical and electronic components on a common substrate, the IC compatible fabrication process we are developing makes the feasibility of subsequent monolithic integration a virtual certainty.

The logical next step in a follow on program to the Thin-Film Optoelectronic Circuits Research Program is the integration of thin-film waveguide devices with an AlGaAs diode laser. The ability to monolithically integrate a laser has formed Honeywell's primary justification for fabricating thin-film ZnO optical circuits on substrates of GaAs rather than silicon. As demonstrated in our Optical Hybrid Gyro program (IR&D), ZnO waveguides can be more easily fabricated on silicon because of its high quality native oxide and superior anisotropic etching properties. The key technical challenge to monolithically integrating an AlGaAs laser with ZnO (or any other) waveguide devices involves developing an on-chip mirror that will facilitate coupling of the laser to an on-chip thin-film waveguide. Two possibilities include ion-etched facets, and grating mirrors such as those used on distributed Bragg reflector (DBR) lasers; the former promises greater ease of coupling to thin-film waveguides.

A second area meriting further investigation is the incorporation of acousto-optic devices with thin-film optoelectronic circuits. Whereas GaAs itself has negligible piezoelectric coefficients, oriented ZnO thin films exhibit a moderately strong piezoelectric effect which can be used to launch surface acoustic waves (SAWs) by means of interdigitated electrode transducers. Optoelectronic circuits relying solely on channel waveguides and electro-optic switches offer high speed operation, but they have been of rather limited complexity because of the large electrode length (millimeters) needed to obtain a sufficient interaction. By contrast, SAW devices, using planar ZnO waveguides, can take advantage of the massive parallelism inherent in optics. Possible devices include the RF spectrum analyzer and the synthetic aperture radar (SAR) processor.

Section V APPENDIX

PROGRAM ORGANIZATION

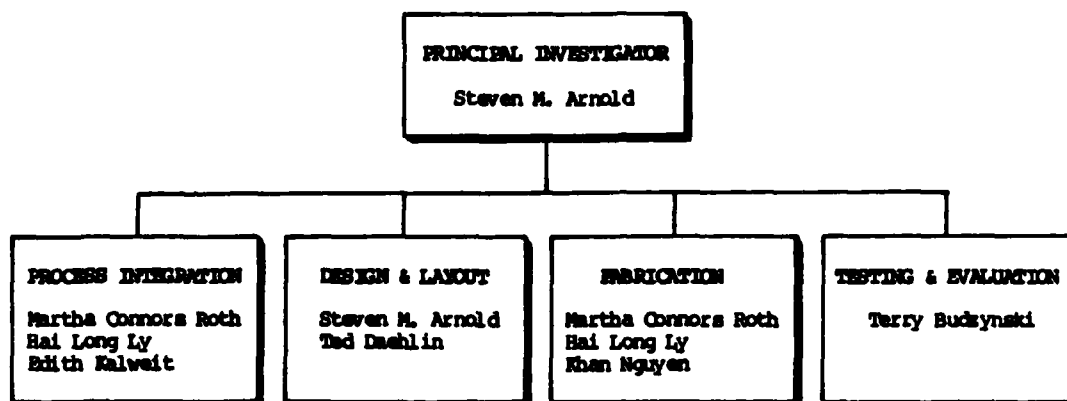


Figure 5-1. Program Organization.

PUBLICATIONS

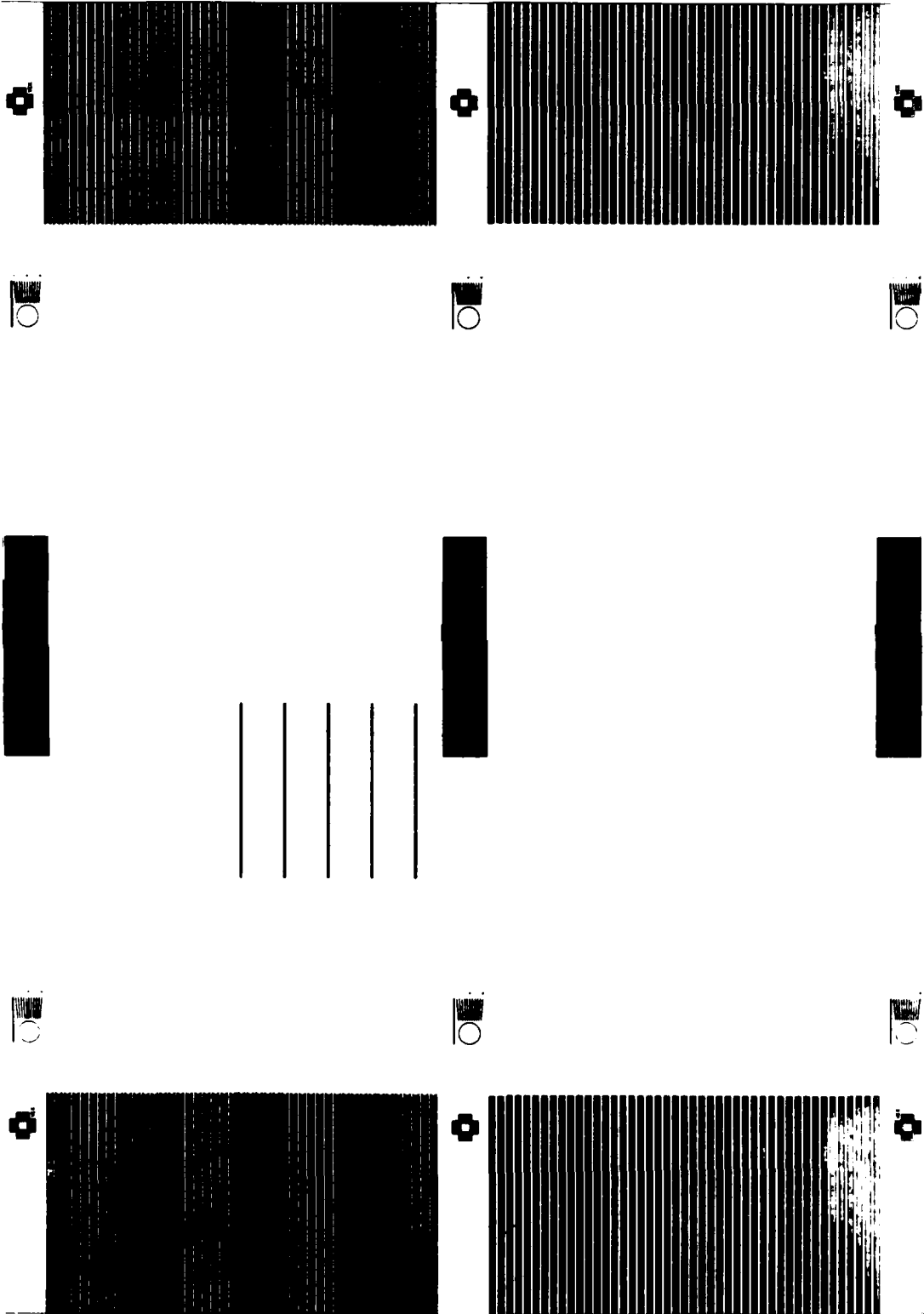
The following patents and publications are anticipated to result from the Thin-Film Optoelectronic Circuits Research Program:

- o Channel Waveguide Schottky Photodiode. A patent disclosure describing our monolithically integrable back-to-back Schottky diode photodetector.
- o Low-Loss Thin-Film Ridge Waveguides on GaAs. A description of our ridge waveguide fabrication procedure and measurements of the excess attenuation loss due to the presence of the ridge structure.
- o Thin-Film ZnO Electro-Optic Switches on GaAs. A report of our Mach-Zehnder interferometric switches and our directional coupler evanescent switches and optical crossbar networks.
- o Monolithically Integrated Schottky Barrier Waveguide Photodetector. A report of our back-to-back Schottky diode photodetector monolithically integrated with thin-film channel waveguides.
- o Coupling of Optical Fibers to Thin-Film Waveguides by GaAs Vee-grooves. A report of our fiber-to-waveguide vee-groove couplers including tapering of the ZnO layer for improved mode matching.

PHASE II MASK SET

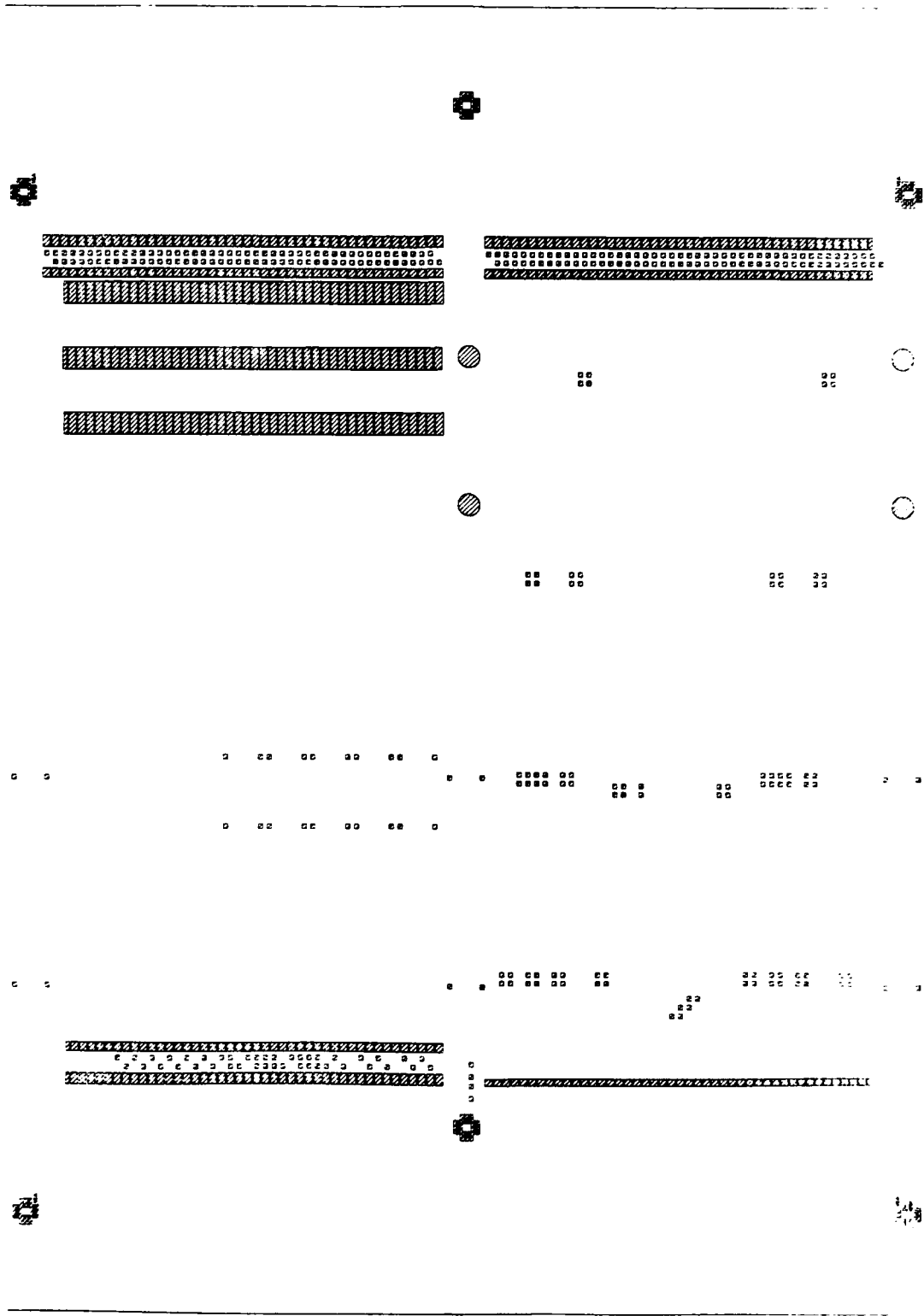
The next several figures are CALMA plots of the six level, Phase II mask set. This e-beam generated mask set is shared equally by the Thin-Film Optoelectronic Circuits Research Program (bottom half, ZnO on GaAs) and the Honeywell-funded Optical Hybrid Gyro Program (top half, ZnO on Si). The decision to share the mask set between two programs was based on a desire to maximize the number of mask design iterations affordable within each program's budget. Overall chip dimensions are 30 mm by 21 mm, of which equal 30 mm by 9 mm areas are devoted to each program and the remaining space (three areas, each 30 mm by 1 mm) contains alignment marks and test patterns. Vee-grooves on 150 micron centers occupy the last 5 mm at each end of the chip, leaving each program with an area of 20 mm by 9 mm for waveguides and active devices.

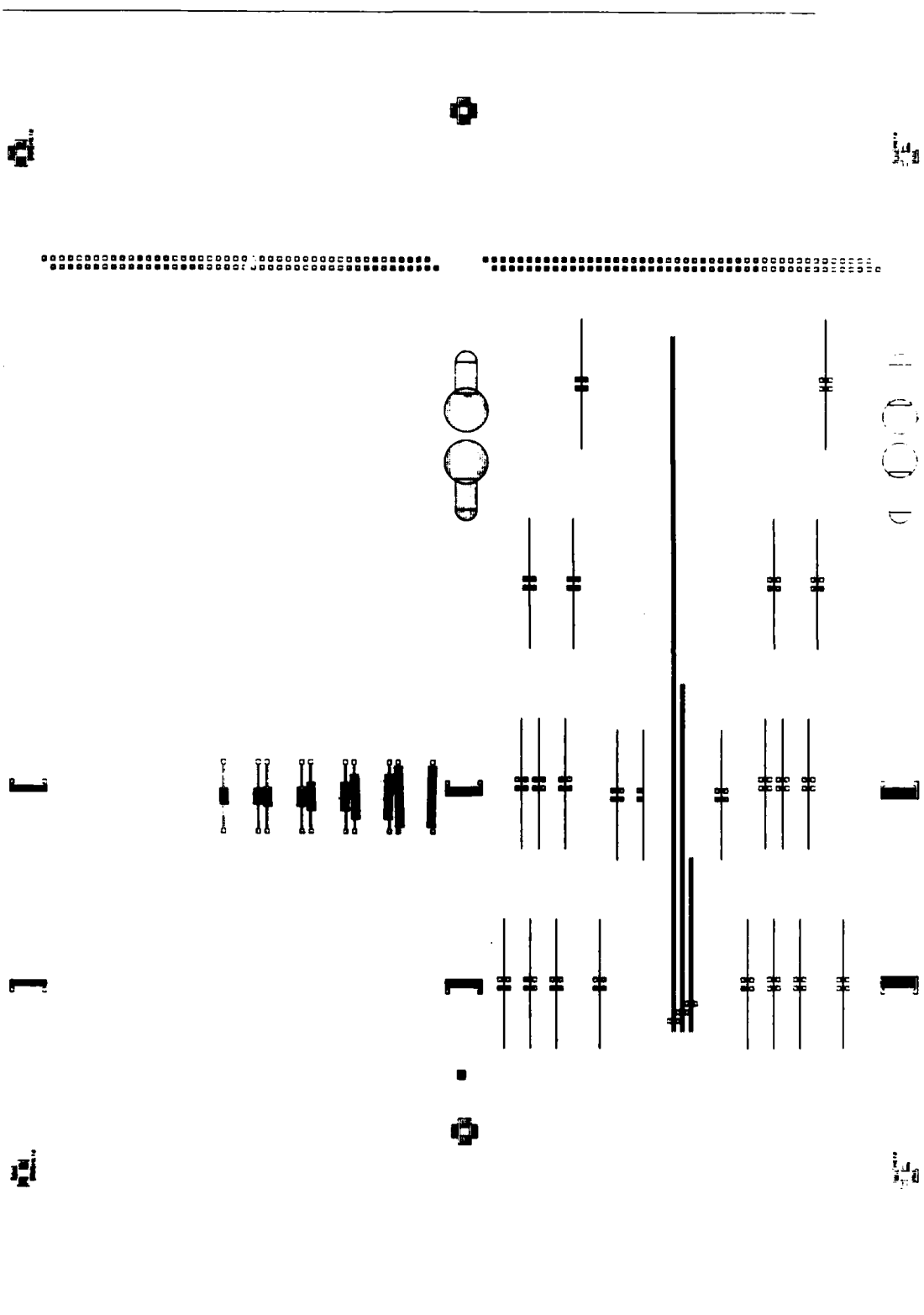
Figure 5-2. Computer Plots of Phase II Mask Set. Following an all-layers plot, plots for individual mask levels are presented in the reverse order from which they occur in the fabrication process (i.e., uppermost layer first).



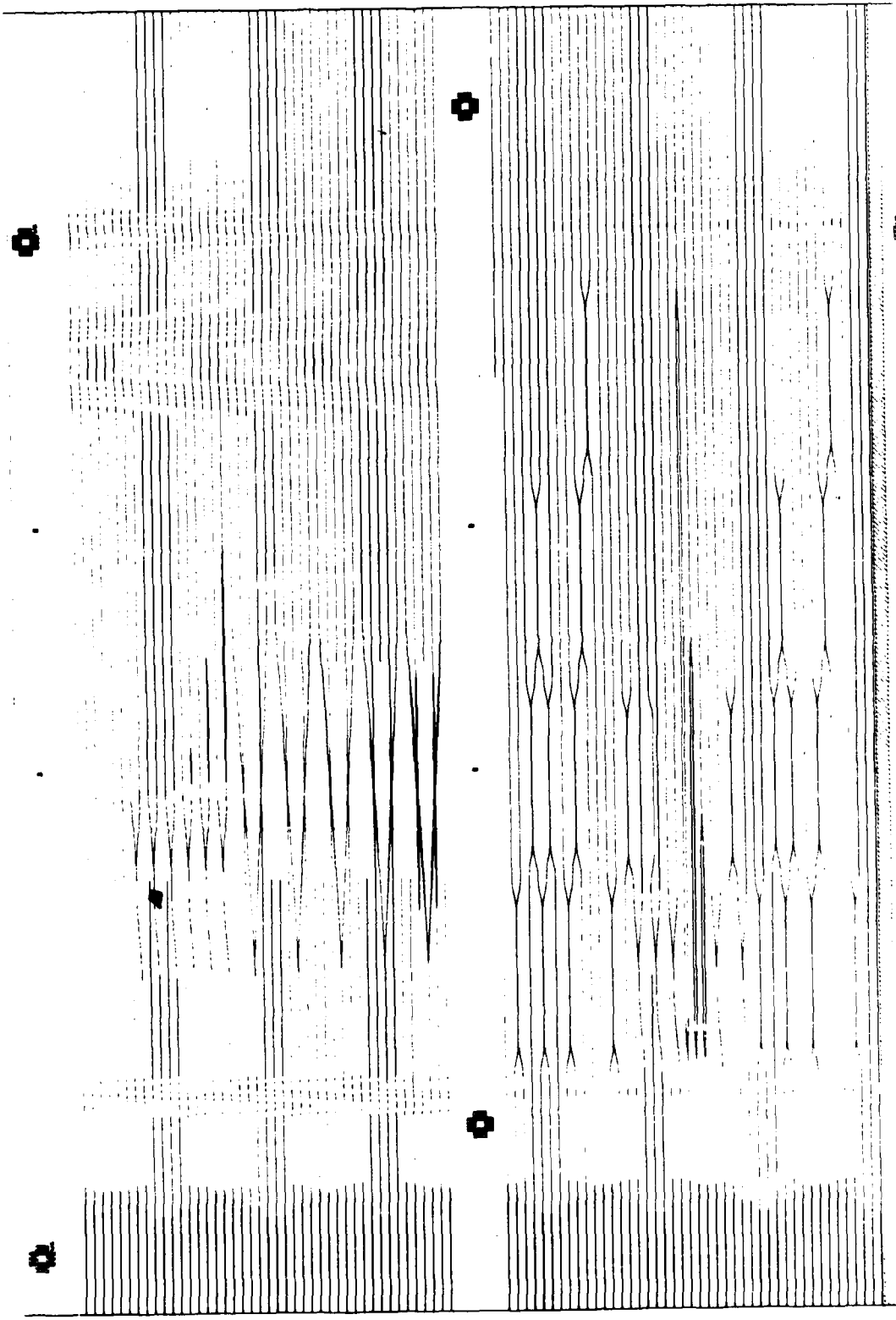
Layer 6 Vee-Grooves

Layer 4 Contact Pads



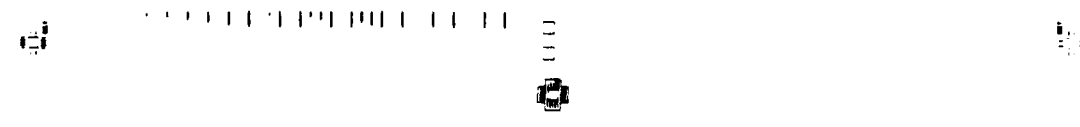
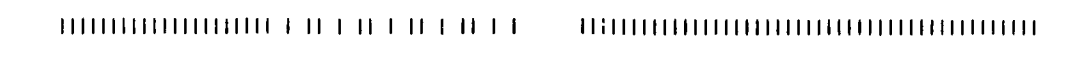
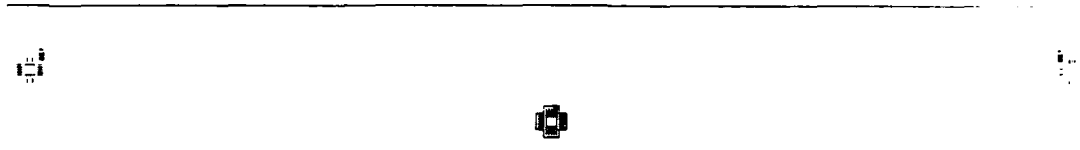


Layer 5 Upper Metalization



Layer 3 Waveguides

100 200 300 400 500 600 700 800 900 1000 1100 1200 1300 1400 1500 1600 1700 1800 1900 2000 2100 2200 2300 2400 2500 2600 2700 2800 2900 3000 3100 3200 3300 3400 3500 3600 3700 3800 3900 4000 4100 4200 4300 4400 4500 4600 4700 4800 4900 5000 5100 5200 5300 5400 5500 5600 5700 5800 5900 6000 6100 6200 6300 6400 6500 6600 6700 6800 6900 7000 7100 7200 7300 7400 7500 7600 7700 7800 7900 8000 8100 8200 8300 8400 8500 8600 8700 8800 8900 9000 9100 9200 9300 9400 9500 9600 9700 9800 9900 10000



Layer 1 Detector Apertures



END

12-86

DTIC